

AD-A952 583

SECRET

1

UNITED STATES NAVY  
AND  
UNITED STATES AIR FORCE  
  
PROJECT SQUID

TECHNICAL REPORT No. 30

DTIC

NOV 10 1983

INFLUENCE OF RESOLVING POWER ON MEASUREMENT  
OF CORRELATIONS AND SPECTRA OF RANDOM FIELDS

PRINCETON UNIVERSITY  
THE JAMES FORRESTAL  
CAMPUS LIBRARY

by

Mahinder S. Uberoi  
Leslie S. G. Kovasznay

ATI-130376

JOHNS HOPKINS UNIVERSITY

DTIC FILE COPY

This document has been approved  
for public release and sale; its  
distribution is unlimited.

83 11 8 201

TECHNICAL REPORT NO. 30

PROJECT SQUID

*A Cooperative Program*

*Of Fundamental Research in Jet Propulsion*

*For The*

*Office of Naval Research, Department of the Navy*

*And The*

*Office of Air Research, Department of the Air Force*

Contract N6-ONR-243, Task Order 20

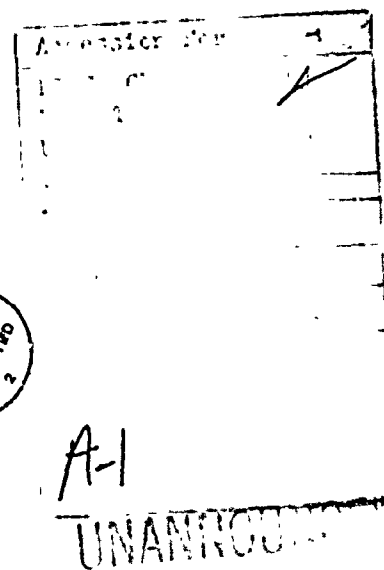
NR 220-088

INFLUENCE OF RESOLVING POWER ON MEASUREMENT  
OF CORRELATIONS AND SPECTRA OF RANDOM FIELDS

by

Mahinder S. Uberoi and Leslie S. G. Kovászna

Johns Hopkins University  
Baltimore, Maryland



This document has been approved for public release and sale; its distribution is unlimited.

## TABLE OF CONTENTS

	Page No.
1. Introduction. . . . .	1
2. General Treatment . . . . .	3
3. Application to turbulence measurement by hot-wire anemometer . . . . .	5
3.1 Terminology for isotropic turbulence. . . . .	5
3.2 Measurement of 'one-dimensional' velocity spectrum . . . . .	6
3.3 Measurement of lateral velocity correlation . . . . .	9
3.4 A simple approximate method of hot-wire length correction for lateral correlation. . .	9
4. Application to scalar random (temperature or density) fields . . . . .	12
4.1 Terminology for random temperature or density fields. . . . .	12
4.2 Hot-wire measurement of random temperature or density fields . . . . .	13
4.3 Shadowgraph method of measuring correlation and spectrum of temperature or density field . . . . .	14
5. Calculations of hot-wire length effect for some simple velocity and temperature spectra .	20
References . . . . .	24
Appendix . . . . .	25
Illustrations . . . . .	27
Distribution List . . . . .	35



# LIST OF SYMBOLS

Greek letters are used to denote measured quantities and Roman letters denote true quantities.

$\mathcal{J}$	linear operator
$K(\bar{s})$	kernel of the operator $\mathcal{J}$
$U_i(\bar{x})$	fluctuating velocity component
$\Omega_i(\bar{x})$	measured fluctuating velocity component
$R_{ij}(\bar{\xi})$	true velocity correlation; $\bar{\xi} = \bar{x}' - \bar{x}$
$\beta_{ij}(\bar{\xi})$	measured velocity correlation
$\psi(\tau)$	'auto-correlation' of the kernel
$S(\bar{k})$	power sensitivity spectrum of $\mathcal{J}$ (the probe)
$E_{ij}(\bar{k})$	Fourier transform of $R_{ij}(\bar{\xi})$
$\Gamma_{ij}(\bar{k})$	Fourier transform of $\beta_{ij}(\bar{\xi})$
$E(k)$	Spectral density of $\sum_i \langle U_i^2 \rangle_{av}$ , with respect to wave-number magnitude
$f(r)$	longitudinal correlation of turbulence.
$g(r)$	lateral correlation of turbulence
$E_1(k_1)$	true 'one-dimensional' velocity spectrum
$\Gamma_1(k_1)$	measured 'one-dimensional' velocity spectrum
$\delta(\bar{\tau})$	Dirac function
$\delta'(\bar{\tau})$	derivative of Dirac function
$\mathcal{W}(\alpha)$	hot-wire length correction weight function for isotropic case
$2l$	length of the hot-wire
$\theta(\bar{x})$	fluctuating temperature
$\rho(\bar{x})$	fluctuating density
$T(\bar{\xi})$	temperature or density correlation
$P(\bar{k})$	Fourier transform of $T(\bar{\xi})$
$G(k)$	spectral density of $\langle \theta^2 \rangle_{av}$ , or $\langle \rho^2 \rangle_{av}$ with respect to wave-number magnitude
$G_1(k_1)$	true 'one-dimensional' density or temperature spectrum
$\gamma_1(k_1)$	measured 'one-dimensional' density or temperature spectrum



$\beta(r)$	measured temperature or density correlation
$B(\bar{x})$	light intensity falling on photographic plate
$h(\bar{x})$	non-dimensional light intensity
$J_0(r)$	Bessel function of zero order
$\Gamma(x)$	Gamma function
$B(z, \gamma)$	Beta function
$\lambda$	the point of intersection of the asymptotes of measured 'one-dimensional' spectrum, when the three-dimensional spectrum is $\sim k^{-n}$
$I$	definite integral $\int_{-\infty}^{\infty} \int_{-\infty}^{\infty} \left( \frac{\sin k_3 l}{k_3} \right)^2 \frac{dk_2 dk_3}{[k_1^2 + k_2^2 + k_3^2]^{3/2}}$

# INFLUENCE OF RESOLVING POWER ON MEASUREMENT OF CORRELATIONS AND SPECTRA OF RANDOM FIELDS

by

Mahinder S. Uberoi and Leslie S. G. Kovásznyay

Johns Hopkins University  
Baltimore, Maryland

## I. INTRODUCTION

1. The experimental techniques used to measure correlations and spectra of random field (e.g. turbulence) use probes with finite extent in space and finite resolution in time. The correlations and spectra are here considered as functions of space variables and time appears as a parameter. We assume that the probe gives faithful response in time and we are concerned with the influence of spatial resolving power of the probe on the measurements of correlations and spectra. Assuming linear response we can consider the probe as a linear operator which maps one random field into another. The problem is to find functional relations between the correlations and spectra of the mapped field to those of the original field. We consider a three-dimensional random vector field with application to turbulence in view; however, from the mathematical point of view the method can be generalized to tensor fields of more than three variables.

## II. GENERAL TREATMENT

$U_i(\bar{x})$  is a random vector field, statistically homogeneous and infinite in extent.  $\Pi$  is the linear operator corresponding to the probe which maps the random field  $U_i(\bar{x})$  into another random field  $\Omega_i(\bar{x})$ . The operator is invariant under a shift in the origin of space.

$$\Pi U_i(\bar{x}) = \Omega_i(\bar{x})$$

$$\Pi U_i(\bar{x} + \bar{\xi}) = \Omega_i(\bar{x} + \bar{\xi})$$

We consider only those operators which can be expressed as a convolution on  $U_i(\bar{x})$  with an arbitrary kernel  $K(\bar{s})$ , i.e.

$$\Pi U_i(\bar{x}) = \int U_i(\bar{x} + \bar{s}) K(\bar{s}) dV(\bar{s})$$

Unless otherwise noted, all integrations are over the whole range of independent variables appearing in the symbol for the volume element. The above definition of an operator includes almost all linear operators of interest if we include Dirac function and its derivatives as possible kernels.\*

Averages are then taken over the entire range of independent variables,

$$\langle U_i(\bar{x}) \rangle_{av.} = \lim_{r \rightarrow \infty} \frac{1}{V(r)} \int_{V(r)} U_i(\bar{x}) dV(\bar{x})$$

where  $V(r)$  is the volume of a sphere of radius  $r$ . We assume  $\langle U_i(\bar{x}) \rangle_{av.}$  are all zero. Space average may be a function of a parameter like time, however, we omit reference to it to avoid an elaborate notation.  $R_{ij}(\bar{\xi})$  and  $\beta_{ij}(\bar{\xi})$  denote correlations of the original and the mapped field respectively.

$$R_{ij}(\bar{\xi}) = \langle U_i(\bar{x}) U_j(\bar{x}') \rangle_{av.}; \quad \bar{x}' = \bar{x} + \bar{\xi}$$

$$\beta_{ij}(\bar{\xi}) = \langle \Omega_i(\bar{x}) \Omega_j(\bar{x}') \rangle_{av.}$$

$E_{ij}(\bar{k})$  and  $\Gamma_{ij}(\bar{k})$  are the spectra of  $U_i(\bar{x})$  and  $\Omega_i(\bar{x})$  respectively,

$$E_{ij}(\bar{k}) = \frac{1}{8\pi^3} \int R_{ij}(\bar{\xi}) e^{i\bar{k} \cdot \bar{\xi}} dV(\bar{\xi})$$

$$\Gamma_{ij}(\bar{k}) = \frac{1}{8\pi^3} \int \beta_{ij}(\bar{\xi}) e^{i\bar{k} \cdot \bar{\xi}} dV(\bar{\xi})$$

\*The operator  $\Pi$  and the kernel  $K$  may be tensors of any rank. A case where tensor operators must be used is the direct measurement of the statistical properties of vorticity by a probe of finite dimensions.

with corresponding inverse relations

$$R_{ij}(\bar{\xi}) = \int E_{ij}(\bar{k}) e^{-i\bar{k} \cdot \bar{\xi}} dV(\bar{k})$$

$$\beta_{ij}(\bar{\xi}) = \int \Gamma_{ij}(\bar{k}) e^{-i\bar{k} \cdot \bar{\xi}} dV(\bar{k})$$

We now investigate relations between  $R_{ij}(\bar{\xi})$ ,  $\beta_{ij}(\bar{\xi})$ ,  $E_{ij}(\bar{k})$  and  $\Gamma_{ij}(\bar{k})$ , the correlations and spectra of the original and the mapped field.

$$\beta_{ij}(\bar{\xi}) = \langle \Omega_i(\bar{x}) \Omega_j(\bar{x}') \rangle_{av.}$$

$$\beta_{ij}(\bar{\xi}) = \lim_{r \rightarrow \infty} \frac{1}{V(r)} \int_{V(r)} dV(\bar{x}) \iint K(\bar{r}) K(\bar{s}) U_i(\bar{x} + \bar{r}) U_j(\bar{x} + \bar{\xi} + \bar{s}) dV(\bar{r}) dV(\bar{s})$$

The integration involving an averaging process and the two integrations with respect to  $\bar{r}$  and  $\bar{s}$  can be interchanged if  $K$  is zero outside of a finite domain or if  $U_i(\bar{x})$  is bounded.

$$\beta_{ij}(\bar{\xi}) = \iint K(\bar{r}) K(\bar{s}) \left[ \lim_{r \rightarrow \infty} \frac{1}{V(r)} \int U_i(\bar{x} + \bar{r}) U_j(\bar{x} + \bar{\xi} + \bar{s}) dV(\bar{x}) \right] dV(\bar{r}) dV(\bar{s})$$

$$= \iint K(\bar{r}) K(\bar{s}) R_{ij}(\bar{\xi} + \bar{s} - \bar{r}) dV(\bar{s}) dV(\bar{r})$$

let  $\bar{r} - \bar{s} = \bar{\tau}$

$$\beta_{ij}(\bar{\xi}) = \iint K(\bar{s}) K(\bar{s} + \bar{\tau}) R_{ij}(\bar{\xi} - \bar{\tau}) dV(\bar{s}) dV(\bar{\tau})$$

Integrate first with respect to  $\bar{s}$  and denote by  $\psi(\bar{\tau})$  the 'auto-correlation' of the kernel  $K$ .

$$\psi(\bar{\tau}) = \int K(\bar{s}) K(\bar{s} + \bar{\tau}) dV(\bar{s}) \quad (2.1)$$

then

$$\beta_{ij}(\bar{\xi}) = \int \psi(\bar{\tau}) R_{ij}(\bar{\xi} - \bar{\tau}) dV(\bar{\tau}) \quad (2.2)$$

Taking Fourier transform of the convolution of  $\psi(\bar{\tau})$  and  $R_{ij}(\bar{\tau})$

$$\Gamma_{ij}(\bar{k}) = S(\bar{k}) E_{ij}(\bar{k}) \quad (2.3)$$

where

$$S(\bar{k}) = \int \psi(\bar{\tau}) e^{-i\bar{k} \cdot \bar{\tau}} dV(\bar{\tau}) \quad (2.4)$$

Since  $\psi(\bar{\tau})$  is an even function,  $S(\bar{k})$  is real and even function of  $\bar{k}$ . We call  $S(\bar{k})$ , the power sensitivity spectrum of  $\mu$ ; it gives the square of the sensitivity of the probe as a function of vector wave number.



It is a multi-dimensional generalization of customary frequency response in circuit analysis. The principal difference is in the fact that time has a preferred direction; on the other hand, space does not necessarily have such a restriction. In circuit analysis  $K(s)$  is the impulse response of the circuit and it acts only on the 'past' of the signal.

### III. APPLICATION TO TURBULENCE MEASUREMENTS BY HOT-WIRE ANEMOMETER

#### 3.1 Terminology for Isotropic Turbulence

We apply the considerations of the last section to isotropic turbulence. For this purpose we introduce the customary terminology.  $U_i(\vec{x})$  is the fluctuating velocity field,  $R_{ij}(\vec{\xi})$  its correlation tensor, and  $E_{ij}(\vec{k})$  its spectral tensor. If the turbulence is isotropic  $R_{ij}(\vec{\xi})$  can be expressed in terms of two scalar functions  $f(r)$  and  $g(r)$ .<sup>1</sup>

$$\begin{aligned} \langle U_i^2 \rangle_{av.} g(r) &= R_{11}(0, r, 0) \\ \langle U_i^2 \rangle_{av.} f(r) &= R_{11}(r, 0, 0) \\ R_{ij}(\vec{\xi}) &= \langle U_i^2 \rangle_{av.} \left\{ \frac{f(r) - g(r)}{r^2} \xi_i \xi_j + g(r) \delta_{ij} \right\}; r^2 = \xi_1^2 + \xi_2^2 + \xi_3^2 \end{aligned} \quad 3.1$$

$R_{ij}(\vec{\xi})$  is an even function of  $\vec{\xi}$ , and it follows that its Fourier transform  $E_{ij}(\vec{k})$  is also an even and real function of  $\vec{k}$ .  $f(r)$  and  $g(r)$  are connected by the continuity equation of incompressible flow.

$$f(r) - g(r) = \frac{-r}{2} \frac{\partial f}{\partial r}$$

Total turbulence intensity

$$\sum_i \langle U_i^2 \rangle_{av.} = R_{ii}(0) = \int E_{ii}(\vec{k}) dV(\vec{k})$$

where repeated index means summation over the index.  $E_{ii}(\vec{k})$  is the spectral density of  $\sum_i \langle U_i^2 \rangle_{av.}$  in the wave-number space. 'Three-dimensional' spectrum  $E(k)$  is the spectral density of  $\sum_i \langle U_i^2 \rangle_{av.}$  with respect to wave-number magnitude

$$E(k) = \int E_{ii}(\vec{k}) d\sigma(k)$$

where  $d\sigma(k)$  is the surface element of a sphere of radius  $k$ . If we apply the conditions of isotropy and continuity equation of incompressible flow to  $E_{ij}(\vec{k})$  and make use of the definition of  $E(k)$  we find<sup>2</sup>

$$E_{ij}(\vec{k}) = \frac{E(k)}{8\pi k^4} [k^2 \delta_{ij} - k_i k_j] \quad 3.2$$

Commonly measured 'one-dimensional' spectrum is the Fourier transform of  $\langle U_i^2 \rangle_{av.} f(r)$ .

$$\begin{aligned} \langle U_i^2 \rangle_{av.} f(r) &= R_{11}(r, 0, 0) = \iiint E_{11}(\vec{k}) e^{-ik_1 r} dk_1 dk_2 dk_3 \\ &= \int E_1(k_1) e^{-ik_1 r} dk_1 \end{aligned}$$

where

$$E_1(k_1) = \int \int E_{11}(\vec{k}) dk_2 dk_3 = \frac{1}{8\pi} \int \frac{E(k)}{k^4} (k_2^2 + k_3^2) dk_2 dk_3$$

$$= \frac{1}{4} \int_{k_1}^{\infty} \frac{E(k)}{k^3} (k^2 - k_1^2) \quad ; \quad k^2 = k_1^2 + k_2^2 + k_3^2 \quad 3.3$$

From which the inverse relation follows:

$$E(k) = 2k^3 \left[ \frac{d}{dk_1} \left( \frac{1}{k_1} \frac{dE_1(k_1)}{dk_1} \right) \right]_{k_1=k}$$

### 3.2 Measurement of 'One-Dimensional' Velocity Spectrum

A hot wire of length  $2\ell$  is set parallel to  $x_3$ ; it is sensitive to  $U_1(\vec{x})$ . The hot-wire output is proportional to the integral of  $U_1(\vec{x})$  over a length  $2\ell$  along the wire. We assume uniform wire temperature distribution that results in uniform velocity response. However, non-uniform temperature distribution offers no essential difficulty. The operator  $\mu$  corresponding to the hot-wire is

$$\Omega_1(\vec{x}) = \mu U_1(\vec{x}) = \int_{-l}^{+l} ds_3 \int \int U_1(\vec{s}) \delta(\vec{s} - \vec{x}) \delta(s_1; s_2) ds_1 ds_2$$

where  $\delta$  stands for a Dirac function. The operator  $\mu$  maps the random field  $U_1(\vec{x})$  into another random field  $\Omega_1(\vec{x})$ . The point of view adopted here is that simultaneous measurements of  $U_1(\vec{x})$  are made at all points in space and we represent these measurements by  $\Omega_1(\vec{x})$ . The spectrum and correlation of  $\Omega_1(\vec{x})$  are related to the spectrum and correlation of  $U_1(\vec{x})$  by 2.2 and 2.3. We first calculate  $\psi(\vec{\tau})$ , the 'auto-correlation' of the kernel  $K$ .

$$\mu U_1(\vec{x}) = \int U_1(\vec{x} + \vec{s}) K(\vec{s}) dV(\vec{s})$$

$$K(\vec{s}) = \begin{cases} \delta(s_1; s_2) \text{ for } & -l \leq s_3 \leq l \\ 0 & \text{otherwise} \end{cases}$$

$$\begin{aligned} \psi(\vec{\tau}) &= \int K(\vec{s}) K(\vec{s} + \vec{\tau}) dV(\vec{s}) \\ &= \int_{-l}^{l} \frac{2\ell - |\tau_3|}{ds_3} \int \int \delta(s_1; s_2) \delta(s_1 + \tau_1; s_2 + \tau_2) ds_1 ds_2 \\ &= \delta(\tau_1; \tau_2) (2\ell - |\tau_3|) \quad -2\ell < \tau_3 < 2\ell \end{aligned} \quad 3.4$$

$S(\vec{k})$ , the power sensitivity spectrum of  $\mu$  is the Fourier transform of  $\psi(\vec{\tau})$

$$\begin{aligned} S(\vec{k}) &= \delta(\tau_1; \tau_2) (2\ell - |\tau_3|) e^{-i\vec{k} \cdot \vec{\tau}} dV(\vec{\tau}) \\ &= 4 \left( \frac{\sin k_3 l}{k_3} \right)^2 \end{aligned}$$

The response of the hot-wire is uniform for  $k_1$  and  $k_2$  and it is poor for large  $k_3 l$ . The graphs of  $\iint K(\bar{s}) d\bar{s}_1 d\bar{s}_2$ ,  $\iint \bar{\psi}(\tau) d\tau_1 d\tau_2$ , and  $s(\bar{k})$  are drawn in Fig. 1.

The relation between  $\Gamma_{11}(\bar{k})$  and  $E_{11}(\bar{k})$  is given by 2.3

$$\begin{aligned}\Gamma_{11}(\bar{k}) &= 4 \left( \frac{\sin k_3 l}{k_3} \right)^2 E_{11}(\bar{k}) \\ &= \frac{1}{2\pi} \left( \frac{\sin k_3 l}{k_3} \right)^2 \frac{E(k)}{k^4} (k_2^2 + k_3^2) \text{ for}\end{aligned}\quad 3.5$$

isotropic turbulence (3.2).

$\Gamma_1(k_1)$  is the 'one-dimensional' spectrum of the mapped field.

$$\begin{aligned}\Gamma_1(k_1) &= \iint \Gamma_{11}(\bar{k}) dk_2 dk_3 \\ &= \frac{1}{2\pi} \iint \left( \frac{\sin k_3 l}{k_3} \right)^2 \frac{E(k)}{k^4} (k_2^2 + k_3^2) dk_2 dk_3\end{aligned}\quad 3.5a$$

let  $\sigma = \sqrt{k_2^2 + k_3^2}$  and  $k_3$  be the new variables.

$$\begin{aligned}\Gamma_1(k_1) &= \frac{2}{\pi} \int_0^\infty \int_0^\sigma \left( \frac{\sin k_3 l}{k_3} \right)^2 \frac{dk_3}{\sqrt{\sigma^2 - k_3^2}} \frac{E(k)}{k^4} \sigma^3 d\sigma \\ &= l^2 \int_{k_1}^\infty W(l \sqrt{k^2 - k_1^2}) \frac{E(k)}{k^3} (k^2 - k_1^2) dk\end{aligned}\quad 3.5b$$

where

$$W(\alpha) = \frac{2}{\pi} \int_0^\alpha \left( \frac{\sin y}{y} \right)^2 \frac{dy}{\sqrt{\alpha^2 - y^2}} \quad 3.6$$

$$W(\alpha) \rightarrow 1 \text{ for } \alpha \ll 1$$

$$\sim \frac{1}{\alpha} \text{ for } \alpha \gg 1$$

$W(\alpha)$  has been numerically integrated and its graph is drawn in Fig. 2. Comparing 3.5b and 3.3 we see that for small  $l$  the measured 'one-dimensional' spectrum  $\Gamma_1(k_1)$  approached the true 'one-dimensional' spectrum  $E_1(k_1)$  except for a factor  $4l^2$  which is the steady state hot-wire response. For large  $l$ ,

$$\frac{\Gamma_1(k_1)}{l} = \int_{k_1}^\infty \frac{E(k)}{k_3} \frac{dk}{\sqrt{k^2 - k_1^2}} \quad 3.7$$

The squared output of the probe is continuously increasing with increasing length of the hot-wire; for the limiting case of infinite wire length the squared out-put per unit length tends to a limit.

$$\Gamma_1'(k_1) = - \int_{k_1}^\infty \frac{E(k)}{k^3} \frac{dk}{\sqrt{k^2 - k_1^2}}$$

For this limiting case the integral equation can be solved explicitly (see Appendix)

$$E(k)_{k=k_1} = \frac{2k_1^2}{l\Pi} \int_{k_1}^{\infty} \Gamma_1''(k) \frac{dk}{\sqrt{k^2 - k_1^2}} \quad 3.8$$

Also

$$\begin{aligned} E_1(k_1) &= \frac{1}{4} \int_{k_1}^{\infty} \frac{E(k)}{k^3} (k^2 - k_1^2) dk \\ &= \frac{1}{2l\Pi} \int_{k_1}^{\infty} \frac{k^2 - k_1^2}{k} dk \int_k^{\infty} \Gamma_1''(\xi) \frac{d\xi}{\sqrt{\xi^2 - k^2}} \end{aligned}$$

integrating first with respect to  $k$ ; then integrating twice by parts, we get

$$E_1(k_1) = \frac{1}{l\Pi} \int_{k_1}^{\infty} \frac{\Gamma_1(\xi) \xi d\xi}{\sqrt{\xi^2 - k_1^2}} \quad 3.9$$

We see that either the 'three-dimensional' spectrum or the true 'one-dimensional' spectrum can be recovered from the spectrum measured by a hot-wire of 'infinite' length. (By 'infinite' length we mean a length much larger than any scale of turbulence). For this limiting case length to diameter ratio of the hot-wire is large and the temperature distribution becomes strictly uniform and independent of the operating conditions, as we have assumed here.

If  $E(k) \sim k^4 \exp \left[ -\frac{k^2}{k_0^2} \right]$   
then  $E_1(k_1) \sim \exp \left[ -\frac{k_1^2}{k_0^2} \right]$  and  $f(r) = \exp \left[ -\frac{r^2 k_0^2}{4} \right]$

where  $k_0$  is a constant. In this case there is no relative distortion of the 'one-dimensional' spectrum or the longitudinal correlation measured with a hot-wire of finite length. Calculations show that

$$\begin{aligned} \frac{\Gamma_1(k_1)}{4\ell^2 E_1(k_1)} &= \frac{\sqrt{\pi}}{2\ell k_0} \operatorname{erf}(k_0 \ell) < 1 \\ &= 1 \text{ for } k_0 \ell \ll 1 \end{aligned}$$

The relation between true and measured intensities of turbulence can be put in terms of the scale of turbulence.

$$\frac{\text{measured}}{\text{true}} \frac{\langle U_1^2 \rangle_{av}}{\langle U_1^2 \rangle_{av}} = \frac{\sqrt{\pi}}{2\ell k_0} \operatorname{erf}(k_0 \ell) = \frac{L_x}{2\ell} \operatorname{erf}\left(\frac{\pi \ell}{L_x}\right)$$

$$\text{where } \frac{\sqrt{\pi}}{k_0} = L_x = \int_{-\infty}^{\infty} f(r) dr^{4.5}$$

In these formulae we have taken account of the fact that the steady state response of the hot-wire is  $4\ell^2$ .

### 3.3 Measurement of Lateral Velocity Correlation

The measured lateral correlation  $\beta_{11}(o, r, o)$  is related to  $R_{11}(o, r, o)$  by 2.2.

$$\beta_{11}(\bar{\xi}) = \int \psi(\bar{\tau}) R_{11}(\bar{\xi} - \bar{\tau}) dV(\bar{\tau})$$

Substitute the value of  $\psi(\bar{\tau})$ , from 3.4

$$\beta_{11}(\xi_1, \xi_2, \xi_3) = \int_{|\tau_3| \leq 2l} \iint \delta(\tau_1, \tau_2) (2l - |\tau_3|) R_{11}(\bar{\xi} - \bar{\tau}) d\tau_1 d\tau_2 d\tau_3$$

Substitute the value of  $R_{11}(\bar{\xi} - \bar{\tau})$  from 3.1

$$\beta_{11}(o, r, o) = \langle U_1^2 \rangle_{av.} \int_{|\tau_3| \leq 2l} (2l - |\tau_3|) g(\sqrt{r^2 + \tau_3^2}) d\tau_3 \quad 3.10$$

This relation was first derived by Skramstad<sup>3</sup>.

If the wire length is much larger than the scale of burbulence, it may be considered effectively infinite, then

$$\frac{\beta_{11}(o, r, o)}{l} = \left[ 4 \int_0^{2l-\infty} g(\sqrt{r^2 + \tau_3^2}) d\tau_3 \right] \langle U_1^2 \rangle_{av.}$$

$$\frac{\beta_{11}(r)}{l} = \left[ 4 \int_0^\infty g(\sqrt{r^2 + \tau_3^2}) d\tau_3 \right] \langle U_1^2 \rangle_{av.}$$

This integral equation can be solved and the true correlation recovered from the measured correlation (see Appendix)

$$\langle U_1^2 \rangle_{av.} g(r) = -\frac{1}{2l\pi} \frac{d}{dr} r \int_0^\infty \frac{\beta_{11}(\sqrt{r^2 + \xi^2})}{r^2 + \xi^2} d\xi \quad 3.11$$

let  $\xi = r \tan \theta$ , then

$$\langle U_1^2 \rangle_{av.} g(r) = -\frac{1}{2l\pi} \frac{d}{dr} r \int_0^{\pi/2} \beta_{11}(r \sec \theta) d\theta \quad 3.12$$

### 3.4 A Simple Approximate Method of Hot-Wire Length Correction for LATERAL Correlation\*

Measurements of lateral correlation  $g(r)$  are often made with hot-wires of inadequate resolving power. We give here an approximate and easy method for correcting the measured correlation taking into account variable temperature along the length of the hot-wire. Hot-wire temperature distribution can be approximated by a parabola  $2/3 - 2/3 (s_s/l)^2$  where  $s_s$  is the distance from the center of the wire along its length. The factor  $2/3$  comes from normalizing the average response to  $4l^2$ . The operator  $\beta_{11}$  corresponding to this

\*This was worked out and used by L. S. G. Kovaszny during the war but has not been published.

hot-wire is

$$H U_1(\bar{x}) = \int_{-l}^{+l} \int \int U_1(\bar{x} + \bar{s}) \left[ \frac{2}{3} - \frac{2}{3} \left( \frac{s_3^2}{l} \right) \right] \delta(s_1; s_2) ds_1 ds_2 ds_3$$

$\psi(\bar{\tau})$  is the 'auto-correlation' of the kernel of the operator  $I'$ .

$$\begin{aligned} \psi(\bar{\tau}) &= l \left\{ 2.4 - 12 \left( \frac{\tau_3}{2l} \right)^2 + 12 \left| \frac{\tau_3}{2l} \right|^3 - 2.4 \left| \frac{\tau_3}{2l} \right|^5 \right\} \delta(\tau_1; \tau_2) \\ &= H(\tau_3) \delta(\tau_1; \tau_2); \text{ (cf 3.4)} \end{aligned}$$

$$\beta_{11}(\bar{\xi}) = \int \psi(\bar{\tau}) R_{11}(\bar{\xi} - \bar{\tau}) dV(\bar{\tau})$$

Substitute the value of  $R_{11}(\bar{\xi} - \bar{\tau})$  from 3.1

$$\beta_{11}(o, r, o) = \langle U_1^2 \rangle_{av} \int_{-2l}^{2l} H(\tau_3) g(\sqrt{r^2 + \tau_3^2}) d\tau_3$$

We normalize the measured correlation  $\beta_{11}(o, r, o)$  to unity for  $r = o$  and denote it by  $\underline{g}(r)$

$$\underline{g}(r) = \frac{\int_0^{2l} H(\tau_3) g(\sqrt{r^2 + \tau_3^2}) d\tau_3}{\int_0^{2l} H(\tau_3) g(\tau_3) d\tau_3}$$

let

$$\tau_3^2 = \eta; \text{ then}$$

$$\begin{aligned} \underline{g}(r) &= \frac{\int_0^{4l^2} H(\eta) g(r^2) \frac{d\eta}{2\sqrt{\eta}} - \int_0^{4l^2} H(\eta) [g(r^2) - g(r^2 + \eta)] \frac{d\eta}{2\sqrt{\eta}}}{\int_0^{4l^2} H(\eta) \frac{d\eta}{2\sqrt{\eta}} - \int_0^{4l^2} [g(o) - g(\eta)] H(\eta) \frac{d\eta}{2\sqrt{\eta}}} \\ &= \frac{g(r^2) - \Delta g(r, l)}{1 - \Delta g(o, l)} \end{aligned}$$

where

$$\Delta g(r, l) = \frac{\int_0^{4l^2} H(\eta) [g(r^2) - g(r^2 + \eta)] \frac{d\eta}{2\sqrt{\eta}}}{\int_0^{4l^2} H(\eta) \frac{d\eta}{2\sqrt{\eta}}}$$

we put

$$g(r^2) - g(r^2 + \eta) \approx [g(r^2) - g(r^2 + 4l^2)] \frac{\eta}{4l^2}$$

then

$$\Delta g(r, l) \approx [g(r^2) - g(r^2 + 4l^2)] \frac{\int_0^{2l} H(\tau_3) \tau_3^2 d\tau_3}{4l^2 \int_0^{2l} H(\tau_3) d\tau_3}$$

$$\approx [g(r^2) - g(r^2 + 4l^2)] \times 0.1$$

$$\approx g(r^2) - g(r^2 + .4l^2)$$

$$\approx \underline{g}(r^2) - \underline{g}(r^2 + .4l^2)$$

For the purpose of calculating the small correction  $\Delta g(r, l)$  we have replaced the true correlation  $g(r^2)$  by the measured correlation  $\underline{g}(r^2)$ . The procedure for applying this approximate length correction to the measured correlation is:

1. Plot the measured correlation  $\underline{g}(r^2)$  against  $r^2$ .
2. Divide the abscissa of this new plot in equal intervals of length  $.4l^2$  (wire length  $= 2l$ ) and find  $\Delta g(r, l)$  (See Fig. 3). The corrected correlation\*

$$\underline{g}(r) = g(r) [1 - \Delta g(o, l)] + \Delta g(r, l)$$

As examples of the corrections involved, we have taken three simple correlations and compared them with measured correlations in Fig. 4. Length of the wire is equal to the microscale in all three cases, i.e.

$2l = \lambda$  and  $\frac{-2}{\lambda^2} = g''(o)$ . This method of correcting the measured correlation is quite good if the length of the wire is not very much larger than the microscale of turbulence.

If

$$\frac{\Delta g(r, l)}{g} = \text{const.}, \quad \frac{dg}{d\eta} = -\frac{1}{\lambda^2} g(\eta) \quad \text{and} \quad g(r) = e^{-\frac{r^2}{\lambda^2}}$$

In this case the simple method gives no correction for the measured correlation coefficient.

---

\*If we assume uniform temperature along the wire then  $\Delta g(r, l) = g(r^2) - g(r^2 + .67l^2)$

According to this approximate method of correcting measured correlation, the relation between the measured intensity and true intensity is,

$$\frac{\text{measured } \langle U_1^2 \rangle_{av.}}{\text{true } \langle U_1^2 \rangle_{av.}} = 1 - \Delta g(o, l) = 1 - [1 - g(.4l^2)] \\ \approx \underline{g(.63l)}$$

#### 4. APPLICATION TO SCALAR RANDOM (TEMPERATURE OR DENSITY) FIELDS

##### 4.1 Terminology for Random Temperature or Density Fields

$\theta(\bar{x})$  is the random temperature field, statistically homogeneous and infinite in extent. We assume that  $\langle \theta(\bar{x}) \rangle_{av.}$  is zero. Let  $T(\bar{\xi})$  and  $P(\bar{k})$  denote correlation and spectrum respectively of the temperature.

$$T(\bar{\xi}) = \langle \theta(\bar{x}) \theta(\bar{x}') \rangle_{av.} ; \bar{x}' = \bar{x} + \bar{\xi}$$

$$P(\bar{k}) = \frac{1}{8\pi^3} \int T(\bar{\xi}) e^{i\bar{k} \cdot \bar{\xi}} dV(\bar{\xi})$$

$$T(\bar{\xi}) = \int P(\bar{k}) e^{i\bar{k} \cdot \bar{\xi}} dV(\bar{k})$$

$P(\bar{k})$  is the spectral density of  $\langle \theta^2(\bar{x}) \rangle_{av.}$  in the wave number space. 'Three-dimensional' spectrum of temperature  $G(k)$  is the spectral density of  $\langle \theta^2(\bar{x}) \rangle_{av.}$  with respect to wave number magnitude

$$G(k) = \int P(\bar{k}) d\sigma(k)$$

$T(r, o, o)$  is the correlation usually measured. The 'one-dimensional' spectrum  $G_1(k_1)$  is the Fourier transform of  $T(r, o, o)$

$$T(r, o, o) = \iiint P(\bar{k}) e^{-ik_1 r} dk_1 dk_2 dk_3 \\ = \int G_1(k_1) e^{-ik_1 r} dk_1$$

where

$$G_1(k_1) = \iint P(\bar{k}) dk_2 dk_3$$

If the random temperature field is statistically homogeneous and isotropic

$$G_1(k_1) = \frac{1}{4\pi} \iint \frac{G(k)}{k^2} dk_2 dk_3$$

$$= \frac{1}{2} \int_{k_1}^{\infty} \frac{G(k)}{k} dk$$

4.1



The inverse relation is

$$G(k) = -2k \left[ \frac{dG_1(k_1)}{dk_1} \right]_{k_1=k} \quad 4.2$$

#### 4.2 Hot-Wire Measurements of Random Temperature or Density Fields

A hot-wire of length  $2l$  is set parallel to  $x_3$ . It is operated at low current such that the heating due to the current is negligible, and it acts as a resistance thermometer. If the current flowing through the wire is constant the voltage fluctuation of the wire is proportional to temperature fluctuation integrated along the length of the wire. The operator  $\Pi$  corresponding to the hot-wire is

$$\Pi \theta(\vec{x}) = \int_{x_3-l}^{x_3+l} \int \int \theta(\vec{x} + \vec{s}) \delta(s_1; s_2) ds_1 ds_2 ds_3$$

Since the mapping operator is the same for temperature and velocity fields, the relations between measured correlations and spectra and the true correlations and spectra are the same for the two cases, except that one is a scalar and the other a vector field. If we denote by  $\gamma_1(k_1)$  the 'one-dimensional' spectrum measured with a hot-wire of length  $2l$ , then (cf 3.5a)

$$\gamma_1(k_1) = 4 \int \int \left( \frac{\sin k_3 l}{k_3} \right)^2 \overline{\rho(k)} dk_2 dk_3$$

for isotropic temperature field,

$$\gamma_1(k_1) = \frac{4}{\pi} \int \int \left( \frac{\sin k_3 l}{k_3} \right)^2 \frac{G(k)}{k^2} dk_2 dk_3$$

let  $\sigma = \sqrt{k_2^2 + k_3^2}$  and  $k_3$  be the new variables, then

$$\gamma_1(k_1) = \frac{4}{\pi} \int_{\sigma=0}^{\infty} \int_0^{\sigma} \left( \frac{\sin k_3 l}{k_3} \right)^2 \frac{dk_3}{\sqrt{\sigma^2 - k_3^2}} \frac{G(k)}{k^2} \sigma d\sigma \quad 4.3$$

$$= 2l^2 \int_{k_1}^{\infty} W(l \sqrt{k^2 - k_1^2}) \frac{G(k)}{k} dk \quad 4.3a$$

where  $W(\alpha)$  is the function introduced in section 2.3.

For small  $\alpha$ ,  $W(\alpha) \approx 1$  and comparison of 4.1 and 4.3 shows that the measured spectrum  $\gamma_1(k_1)$  approaches the true spectrum  $G_1(k_1)$  except for a factor  $\frac{1}{k^2}$  which is the steady state response of the hot-wire.

For large  $l$ ,  $W(l \sqrt{k^2 - k_1^2}) \approx \frac{1}{l \sqrt{k^2 - k_1^2}}$  and

$$\gamma_1(k_1) = 2l \int_{k_1}^{\infty} \frac{G(k)}{k} \frac{dk}{\sqrt{k^2 - k_1^2}} \quad 4.4$$

For this limiting case the integral equation can be solved explicitly (see Appendix)

$$G(k)_{k=k_1} = -\frac{1}{l\pi} \int_{k_1}^{\infty} \left[ k \gamma_1(k) \right]' \frac{k dk}{\sqrt{k^2 - k_1^2}} \quad 4.4a$$

Also

$$\begin{aligned} G_1(k_1) &= \frac{1}{2} \int_{k_1}^{\infty} \frac{G(k)}{k} dk \\ &= -\frac{1}{2l\pi} \int_{k_1}^{\infty} \frac{dk}{k} \int_k^{\infty} \frac{[\xi \gamma_1(\xi)]' \xi d\xi}{\sqrt{\xi^2 - k^2}} \end{aligned}$$

Integrating first with respect to  $k$  and then once by parts we get

$$G_1(k_1) = \frac{1}{4\pi l} \int_{k_1}^{\infty} \gamma_1(\xi) \frac{\xi d\xi}{\sqrt{\xi^2 - k_1^2}} \quad 4.4b$$

If

$$G(k) \sim k^2 \exp \left[ -\frac{k^2}{k_0^2} \right]$$

then

$$G_1(k_1) \sim \exp \left[ -\frac{k_1^2}{k_0^2} \right]$$

where  $k_0$  is a constant, and for this case there is no relative distortion of 'one-dimensional' spectrum measured with a hot-wire of finite length. Calculations show that

$$\begin{aligned} \frac{\gamma_1(k_1)}{4l^2 G_1(k_1)} &= \frac{\sqrt{\pi}}{lk_0} \operatorname{erf}(lk_0) - \frac{1}{l^2 k_0^2} \left[ \exp(-l^2 k_0^2) - 1 \right] < 1 \\ &\approx 1 \text{ for } lk_0 \ll 1 \end{aligned}$$

#### 4.3 Shadowgraph Method of Measuring Correlation and Spectrum of Random Temperature or Density Fields\*

$\rho(\vec{x})$  is the fluctuating random density field, statistically homogeneous and infinite in extent. We assume that  $\langle \rho(\vec{x}) \rangle_{av.}$  is zero. A portion of the field, lying between  $x_3 - l$  and  $x_3 + l$  and extending to infinity in the other two directions, is removed from the rest of the field. Parallel light after passing through this slab of the field is incident on a photographic plate (Fig. 5). The light arriving at the plate will be more or less intense according to the distortion produced by density fluctuations acting as concave or convex lenses. The shadowgraph depends on the position of the slab relative to  $x_3$  axis. A single shadowgraph gives the mapped field for a fixed value of  $x_3$  and the complete mapping consists of a continuous set of shadowgraphs, one for each value of  $x_3$ .

\*This is the extension of the work reported by one of us in reference 9.

For small fluctuations of density, the refractive index  $\mu$  is a linear function of  $\rho$ ,  $\mu = 1 + c\rho$ , where  $c$  is a constant. If the photographic plate is placed closer than the first focal point there are no singular points on the photographic plate. The light intensity  $B(x_1, x_2, x_3)$  falling on the plate compared to the intensity  $B_0$  of the incident light is <sup>6</sup>

$$h(x_1, x_2, x_3) = \frac{B_0 - B(x_1, x_2, x_3)}{B(x_1, x_2, x_3)} = \int_{x_3-l}^{x_3+l} \left( \frac{\partial^2 \rho}{\partial x_1^2} + \frac{\partial^2 \rho}{\partial x_2^2} \right) dx_3 \quad 4.5$$

We have omitted the dimensional constant in the above relation. Since we have assumed statistically homogeneous field, the statistical properties of  $h(x_1, x_2, x_3)$  with  $x_1$  and  $x_2$  as variables are independent of  $x_3$ . Let

$$\beta(\xi_1, \xi_2, 0) = \langle h(x_1, x_2, x_3) h(x_1 + \xi_1, x_2 + \xi_2, x_3) \rangle_{av}.$$

This correlation can be obtained from the shadowgraph. For this purpose two slides are made from the shadowgraph and placed face to face. The combined pattern is the same as for a single slide if the position of two plates is matched. If  $t(x_1, x_2, x_3)$  is the transparency of either plate, the transparency of two plates displaced from the matched position by amounts  $\xi_1$  and  $\xi_2$  is

$$t_2 = t(x_1, x_2, x_3) t(x_1 + \xi_1, x_2 + \xi_2, x_3)$$

Let  $t(x_1, x_2, x_3) = t_0 + \Delta t(x_1, x_2, x_3)$  where  $t_0$  is the average transparency. The fluctuating transparency  $\Delta t(x_1, x_2, x_3) = ch(x_1, x_2, x_3)$  where  $c$  is a constant, if the photographic process is linear. Making use of this relation and taking averages of  $t_2$  we find,

$$\begin{aligned} \langle t_2 \rangle_{av} &= t_0^2 + c \langle h(x_1, x_2, x_3) h(x_1 + \xi_1, x_2 + \xi_2, x_3) \rangle_{av} \\ &= t_0^2 + c \beta(\xi_1, \xi_2, 0) \end{aligned} \quad 4.6$$

We can determine  $\beta(\xi_1, \xi_2, 0)$  by measuring combined transparency of two plates.

The operator  $\Pi$  which maps the random density field  $\rho(\vec{x})$  into another random field  $h(\vec{x})$  is, (cf 4.5).

$$h(\vec{x}) = \Pi \rho(\vec{x}) = \int_{-l}^{+l} \int \int \rho(\vec{x} + \vec{s}) \left\{ \delta''(s_1) \delta(s_2) + \delta''(s_2) \delta(s_1) \right\} ds_1 ds_2 ds_3$$

$\psi(\bar{\tau})$  is the 'auto-correlation' of the kernel of the operator  $\mathcal{H}$

$$\begin{aligned} \psi(\bar{\tau}) = & \int_{-l}^{+l} \int \left\{ \delta''(s_1) \delta(s_2) + \delta''(s_2) \delta(s_1) \right\} \left\{ \delta''(s_1 + \tau_1) \delta(s_2 + \tau_2) \right. \\ & \left. + \delta''(s_2 + \tau_2) \delta(s_1 + \tau_1) \right\} ds_1 ds_2 ds_3 \\ \psi(\bar{\tau}) = & \left\{ \delta^{iv}(\tau_1) \delta(\tau_2) + \delta^{iv}(\tau_2) \delta(\tau_1) + 2 \delta''(\tau_1) \delta''(\tau_2) \right\} (2l - |\tau_3|) \end{aligned} \quad 4.7$$

$S(\bar{k})$  is the power sensitivity spectrum of  $\mathcal{H}$   $|\tau_3| \leq 2l$

$$\begin{aligned} S(\bar{k}) = & \int \psi(\bar{\tau}) l^{-i\bar{k} \cdot \bar{\tau}} dV(\bar{\tau}) \\ = & 4(k_1^2 + k_2^2)^2 \left( \frac{\sin k_3 l}{k_3} \right)^2 \end{aligned} \quad 4.8$$

The shadowgraph method responds to second derivatives of the density field; this accounts for the factor  $(k_1^2 + k_2^2)^2$ . Since the light passes through a path  $2l$  (which corresponds to a hot-wire of length  $2l$  in the previous example of velocity spectrum measurement) the factor  $4 \left( \frac{\sin k_3 l}{k_3} \right)^2$  appears in the sensitivity spectrum.

The notation for correlation and spectrum of  $\rho(\bar{x})$  is the same as for random temperature field  $\theta(\bar{x})$  developed in Section 4.1, i.e.,

$$T(\bar{\xi}) = \langle \rho(\bar{x}) \rho(\bar{x}') \rangle_{av}, \quad \bar{x}' = \bar{x} + \bar{\xi}$$

$$P(\bar{k}) = \frac{1}{8\pi^3} \int T(\bar{\xi}) e^{i\bar{k} \cdot \bar{\xi}} dV(\bar{\xi})$$

$$T(\bar{\xi}) = \int P(\bar{k}) e^{-i\bar{k} \cdot \bar{\xi}} dV(\bar{k})$$

and  $G(\bar{k})$  is the 'three-dimensional' spectrum of  $\rho(\bar{x})$

$$G(\bar{k}) = \int P(\bar{k}) d\sigma(\bar{k})$$

If

$$\Gamma(\bar{k}) = \frac{1}{8\pi^3} \int \beta(\bar{\xi}) e^{i\bar{k} \cdot \bar{\xi}} dV(\bar{\xi})$$

then

$$\Gamma(\bar{k}) = S(\bar{k}) P(\bar{k})$$

$$= 4 (k_1^2 + k_2^2)^2 \left( \frac{\sin k_3 l}{k_3} \right)^2 P(\bar{k})$$

for isotropic random density field

$$= 4 (k_1^2 + k_2^2)^2 \left( \frac{\sin k_3 l}{k_3} \right)^2 \frac{1}{4\pi} \frac{G(k)}{k^2} \quad 4.10$$

and

$$\beta(\bar{\xi}) = \frac{1}{\pi} \int \frac{G(k)}{k^2} (k_1^2 + k_2^2)^2 \left( \frac{\sin k_3 l}{k_3} \right)^2 e^{-i\bar{k} \cdot \bar{\xi}} dV(\bar{k}) \quad 4.11$$

$$\beta(\xi_1, \xi_2, 0) = \frac{1}{\pi} \iiint \left( \frac{\sin k_3 l}{k_3} \right)^2 \frac{G(k)}{k^2} (k_1^2 + k_2^2)^2 e^{-i(k_1 \xi_1 + k_2 \xi_2)} dk_1 dk_2 dk_3$$

If  $l$  is much larger than any scale of turbulence, then  $\left( \frac{\sin k_3 l}{k_3} \right)^2$  acts almost like a Dirac function, i.e. we can replace  $\frac{G(k)}{k^2}$  by  $\frac{G(\sqrt{k_1^2 + k_2^2})}{k_1^2 + k_2^2}$  and integrate with respect to  $k_3$ . Under this assumption

$$\frac{\beta(\xi_1, \xi_2, 0)}{l} = \iint G(\sqrt{k_1^2 + k_2^2}) (k_1^2 + k_2^2) e^{-i(k_1 \xi_1 + k_2 \xi_2)} dk_1 dk_2 \quad 4.12$$

Introduce polar coordinates,

$$\xi_1 = r \cos \zeta ; k_1 = \nu \cos \psi$$

$$\xi_2 = r \sin \zeta ; k_2 = \nu \sin \psi$$

$$\beta(r) = 2\pi l \int_0^\infty \nu^3 G(\nu) J_0(\nu r) d\nu \quad 4.12a$$

and the inverse relation,

$$\nu^2 G(\nu) = \frac{1}{2\pi l} \int_0^\infty r \beta(r) J_0(\nu r) dr \quad 4.12b$$

The measured correlation  $\beta(r)$  and  $\nu^2 G(\nu)$  are Fourier-Bessel transforms of each other.<sup>3</sup> For  $\nu \ll 1$ ;  $\nu^2 G(\nu) \sim \nu^4$  making the first and the third moments of  $\beta(r)$  always zero. The relation between the conventional correlation  $T(\bar{\xi})$  and the correlation of the shadowgraph is given by eq. 2.2

$$\beta(\bar{\xi}) = \int \psi(\bar{\tau}) T(\bar{\xi} - \bar{\tau}) d\bar{\tau}$$

Substitute  $\psi(\bar{\tau})$  from equation 4.7 and integrate with respect to  $\tau_1$  and  $\tau_2$

$$\beta(\bar{\xi}) = \int_{-l}^l \left( \frac{\partial^4}{\partial \xi_1^4} + \frac{2\partial^4}{\partial \xi_1^2 \partial \xi_2^2} + \frac{\partial^4}{\partial \xi_2^4} \right) (2l - |\tau_3|) T(\bar{\xi} - \bar{\tau}) d\tau_3$$

For isotropic density fluctuations

$$\begin{aligned}\beta(\sqrt{\xi_1^2 + \xi_2^2}) &= 2 \int_0^{2l} (2l - \tau_3) \Delta_\xi^2 T(\sqrt{\xi_1^2 + \xi_2^2 + \tau_3^2}) d\tau_3 \\ \beta(r) &= 2 \int_0^{2l} (2l - \tau_3) \Delta_r^2 T(\sqrt{r^2 + \tau_3^2}) d\tau_3\end{aligned}\quad 4.13$$

where  $\Delta_r^2$  is the bilaplacian in two dimensions for circularly symmetric case.

If  $l$  is much larger than any scale of density fluctuations, then

$$\frac{\beta(r)}{l} = 4 \int_0^{2l} \Delta_r^2 T(\sqrt{r^2 + \tau_3^2}) d\tau_3 \quad 4.13a$$

$$\frac{\beta(r)}{l} = \Delta_r^2 \phi(r) \quad 4.13b$$

$r^2 \log r$  is the elementary solution of bilaplacian in two dimensions<sup>7</sup>.

If we assume that  $T(r) \underset{r \rightarrow \infty}{\sim} \frac{1}{r^\epsilon}$ ;  $\epsilon > 0$  then the solution of 4.13b is

$$\begin{aligned}\phi(r) &= \frac{1}{18\pi} \int_0^\infty \int_0^{2\pi} \beta(\xi) (r^2 + \xi^2 - 2r\xi \cos \theta) \log \sqrt{r^2 + \xi^2 - 2r\xi \cos \theta} \xi d\theta d\xi \\ &= \frac{1}{4} \int_0^r \beta(\xi) \xi [(r^2 + \xi^2) \log r + \xi^2] d\xi + \frac{1}{4l} \int_r^\infty \beta(\xi) [\xi (r^2 + \xi^2) \log \xi + r^2] d\xi\end{aligned}$$

We note that first and third moments of  $\beta(\xi)$  are zero, using this fact:

$$\phi(r) = -\frac{1}{4l} \int_r^\infty \beta(\xi) \xi [(r^2 + \xi^2) \log r + \xi^2] d\xi + \frac{1}{4l} \int_r^\infty \beta(\xi) \xi [(r^2 + \xi^2) \log \xi + r^2] d\xi$$

substitute for  $\phi(r)$  from 4.13a

$$\begin{aligned}\phi(r) &= 4 \int_0^\infty T(\sqrt{r^2 + \tau_3^2}) d\tau_3 \\ &= \frac{1}{4l} \int_r^\infty \beta(\xi) \xi [(r^2 + \xi^2) (\log \xi - \log r) + r^2 - \xi^2] d\xi\end{aligned}$$

This integral equation can be solved for  $T(r)$  (see Appendix)

$$\begin{aligned} r^2 T(r) &= -\frac{1}{2\pi} \int_r^\infty \left[ \phi(s) + \phi'(s) s \right] \frac{s ds}{s^2 - r^2} \\ &= -\frac{1}{8l\pi} \int_r^\infty \int_s^\infty \beta(\xi) \xi [(3s^2 + \xi^2)(\log \xi - \log s) + 2s^2 - 2\xi^2] \frac{s ds}{s^2 - r^2} d\xi \end{aligned}$$

integrate first with respect to  $s$ .

$$\begin{aligned} r^2 T(r) &= -\frac{1}{8l\pi} \int_r^\infty \beta(\xi) \xi d\xi \int_r^\xi [(3s^2 + \xi^2)(\log \xi - \log s) + 2s^2 - 2\xi^2] \frac{s ds}{s^2 - r^2} \\ T(r) &= \frac{1}{8l\pi} \int_r^\infty \beta(\xi) \xi \lambda(\xi, r) d\xi \end{aligned} \quad 4.14$$

where

$$\begin{aligned} \lambda(\xi, r) &= -\frac{1}{r^2} \int_r^\xi [(3s^2 + \xi^2)(\log \xi - \log s) + 2s^2 - 2\xi^2] \frac{s ds}{s^2 - r^2} \\ &= \left( \frac{2r^2 + \xi^2}{r} \right) \cos^{-1} \left| \frac{r}{\xi} \right| - 3 \sqrt{\xi^2 - r^2} \end{aligned} \quad 4.15$$

In order to get a feeling for the correlation measured from the shadowgraph, we assume that

$G(k) \sim k^2 \exp \left[ -\frac{\lambda_\rho^2 k^2}{4} \right]$  then it follows that the conventional correlation

$$T(r) \sim \exp \left[ -(r/\lambda_\rho)^2 \right]$$

and

$$\beta(r) \sim \left[ 1 - 2 \left( \frac{r}{\lambda_\rho} \right)^2 + \frac{1}{2} \left( \frac{r}{\lambda_\rho} \right)^4 \right] \exp \left[ -\left( \frac{r}{\lambda_\rho} \right)^2 \right]$$

where  $\lambda_\rho = -\frac{2T(0)}{T''(0)}$  and  $\lambda_\rho$  is a characteristic length similar to turbulence micro-scale, we may call it density micro-scale. These correlations are normalized to unity for  $r=0$  and compared in Fig. 6.

We denote by  $\gamma_1(k_1)$  the 'one-dimensional' spectrum of the mapped field.

$$\begin{aligned} \gamma_1(k_1) &= \iint \Gamma(\vec{k}) dk_2 dk_3 \\ &= \frac{1}{\pi} \iint (k_1^2 + k_2^2)^2 \left( \frac{\sin k_3 l}{k_3} \right)^2 \frac{G(k)}{k^2} dk_2 dk_3 \end{aligned}$$

For the case of 'infinitely long' light path, we can simplify this expression (cf. 4.12)

$$\begin{aligned} \gamma_1(k_1) &= l \int (k_1^2 + k_2^2) G(\sqrt{k_1^2 + k_2^2}) dk_2 \\ &= l \int_{k_1}^\infty k^3 G(k) \frac{dk}{\sqrt{k^2 - k_1^2}} \end{aligned} \quad 4.16$$

$\gamma_1(k_1)$  is the 'one-dimensional' spectrum of the shadowgraph for the limiting case of 'infinite' light path. This spectrum can be measured by scanning the shadowgraph with a beam of light. In the case of low level wind-tunnel turbulence we can assume that density pattern is carried along by the mean stream. Parallel light after passing through the density field is allowed to fall through a narrow hole on a photo-cell and the output of the photo-cell is analyzed by electrical filter. Using the relation  $x = Ut$  where  $U$  is the mean velocity the measured time spectrum can be converted into space spectrum. 'Three-dimensional' spectrum can be recovered from the measured spectrum by solving eq. 4.16 (see Appendix).

$$G(k)_{k=k_1} = - \frac{2}{k_1^4 l \pi} \int_{k_1}^{\infty} [k \gamma_1(k)]' \frac{k dk}{\sqrt{k^2 - k_1^2}} \quad 4.17$$

Also

$$\begin{aligned} G_1(k_1) &= \frac{1}{2} \int_{k_1}^{\infty} \frac{G(k)}{k} dk \\ &= - \frac{1}{l \pi} \int_{k_1}^{\infty} \frac{dk}{k^5} \int_k^{\infty} \frac{[\xi \gamma_1(\xi)]' \xi}{\sqrt{\xi^2 - k^2}} d\xi \end{aligned} \quad 4.18$$

integrate first with respect to  $k$

$$\begin{aligned} &= \frac{1}{l \pi} \int_{k_1}^{\infty} \xi [\xi \gamma_1(\xi)]' d\xi \int_{k_1}^{\xi} \frac{dk}{k^5 \sqrt{\xi^2 - k^2}} \\ G_1(k_1) &= \frac{1}{l \pi} \int_{k_1}^{\infty} \gamma_1(\xi) \left[ \frac{3k_1^2 - \xi^2}{2 \xi^3 k_1^2 \sqrt{\xi^2 - k_1^2}} - \frac{3}{4 \xi^4} \log \frac{\xi + \sqrt{\xi^2 - k_1^2}}{k_1} \right] d\xi \end{aligned} \quad 4.19$$

We can also use Schlieren instead of shadow method to measure correlation and spectrum of random density field. If we assume that the light path is larger than scale of density fluctuations then true correlation and spectrum of density fluctuations can be recovered from the measured quantities in the same way as in the case of shadowgraph.

##### 5. Calculation of Hot-Wire Length Effect for Some Simple Velocity and Temperature Spectra

In order to get an idea about the hot-wire length effect we assume that  $E(k) = k^{-n}$ . The 'one-dimensional' velocity spectrum measured with a hot-wire of length  $2l$  is compared with true spectrum in Fig. 7. Explicit calculations are made as follows:

$$\begin{aligned} \Gamma_1(k_1; n) &= l^2 \int_{k_1}^{\infty} W(l \sqrt{k^2 - k_1^2}) k^{-(n+3)} (k^2 - k_1^2) dk \\ &\approx l^2 \int_{k_1}^{\infty} k^{-(n+3)} (k^2 - k_1^2) dk \text{ for } lk_1 \ll 1 \\ &\approx l^2 \frac{k_1^{-n}}{2} \int_0^{\infty} \frac{s ds}{(1+s)^{\frac{n}{2}+1}} ; s = \frac{k^2 - k_1^2}{k_1^2} \\ &\approx l^2 \frac{k_1^{-n}}{2} B\left(\frac{n}{2}, 2\right) \end{aligned} \quad 5.1$$



for

$$lk_1 \gg 1, W(l \sqrt{k^2 - k_1^2}) \approx \frac{1}{l \sqrt{k^2 - k_1^2}}$$

and

$$\begin{aligned} \Gamma_1(k_1; n) &= l \int_{k_1}^{\infty} K^{-(n+3)} \sqrt{k^2 - k_1^2} dk \\ &\approx l \frac{k - (n+1)}{2} \int_0^{\infty} \frac{\sqrt{s} ds}{(1+s)^{\frac{n}{2}+2}} \\ &\approx l \frac{k_1^{n+1}}{2} B\left(\frac{3}{2}, \frac{n+1}{2}\right) \end{aligned} \quad 5.2$$

The point of intersection of asymptotes 5.1 and 5.2 is

$$\begin{aligned} \Delta = 2lk_1 &= \frac{2B\left(\frac{3}{2}, \frac{n+1}{2}\right)}{B\left(\frac{n}{2}, 2\right)} \\ &= \frac{2\Gamma\left(\frac{3}{2}\right)\Gamma\left(\frac{n+1}{2}\right)}{\Gamma\left(\frac{n}{2}\right)} \end{aligned} \quad 5.3$$

The graph of equation 5.3 is drawn in Fig. 8. The complete calculation of  $\Gamma_1(k_1; 1)$  can be made by taking it in the form

$$\Gamma_1(k_1; 1) = \frac{1}{3\pi} \iint 4 \left( \frac{\sin k_3 l}{k_3} \right)^2 \frac{(k_1^2 + k_3^2)}{(k_1^2 + k_2^2 + k_3^2)^{3/2}} dk_2 dk_3 \quad 5.4$$

$$\begin{aligned} &= \frac{1}{2\pi} \iint \left( \frac{\sin k_3 l}{k_3} \right)^2 \frac{dk_2 dk_3}{(k_1^2 + k_2^2 + k_3^2)^{3/2}} - \frac{k_1^2}{2\pi} \iint \left( \frac{\sin k_3 l}{k_3} \right)^2 \frac{dk_2 dk_3}{(k_1^2 + k_2^2 + k_3^2)^{3/2}} \\ &= \frac{l}{2\pi} + \frac{k_1}{6\pi} \frac{\partial l}{\partial k_1} \end{aligned} \quad 5.5$$

where

$$\begin{aligned} l &= \iint \left( \frac{\sin k_3 l}{k_3} \right)^2 \frac{dk_2 dk_3}{(k_1^2 + k_2^2 + k_3^2)^{3/2}} \\ &= 2 \int_0^{\infty} \left( \frac{\sin k_3 l}{k_3} \right)^2 \frac{dk_3}{k_1^2 + k_3^2} \end{aligned}$$

We evaluate this integral using Parseval's relation. Take Fourier transforms of  $\left( \frac{\sin k_3 l}{k_3} \right)^2$  and  $\frac{l}{k_1^2 + k_3^2}$  and integrate the product of the transforms with respect to the variable of transformation.

$$I = 2 \int_{-2l}^{2l} \left\{ \sqrt{\frac{\pi}{2}} \left( \frac{2l - |x|}{2} \right) \right\} \left\{ \frac{\sqrt{\pi}}{2} \frac{1}{k_1} \exp(-|xk_1|) \right\} dx$$

$$= \pi (2l/k_1^2 - 1/k_1^3 + 1/k_1^3 \exp[-2lk_1])$$

Substitute the value of I in 5.5

$$\Gamma_1(k_1; 1) = \frac{1}{3} \left( \frac{l}{k_1^2} - \frac{l}{k_1^2} \exp[-2lk_1] \right) \quad 5.6$$

$\Gamma_1(k_1; n)$  for  $n=3, 5, 7$  can be obtained by differentiating  $\Gamma_1(k_1; 1)$  with respect to  $k_1$

$$\frac{\partial \Gamma_1(k_1; 1)}{\partial k_1} = -5k_1 \Gamma_1(k_1; 3) \quad 5.7$$

The ratio of measured spectrum  $\Gamma_1(k_1; n)$  to the true spectrum at the point of intersection of the two asymptotes of  $\Gamma_1(k_1; n)$  is plotted against  $n$  for  $n = 1, 3, 5, \dots$  in Fig. 9. A smooth curve is drawn through these points. Knowing the asymptotic value of  $\Gamma_1(k_1; n)$  for  $2lk_1 \ll 1$  and  $2lk_1 \gg 1$  and its value at the intersection of the asymptotes we can draw approximately the complete curve of  $\Gamma_1(k_1; n)$  for all  $n$ . Graphs of the ratio of measured spectrum to the true spectrum are drawn against the non-dimensional variable  $2lk_1$  in Fig. 10.

If we assume that  $G(k) = k^{-n}$  then the 'one-dimensional spectrum of temperature measured with a hot-wire of length  $2l$  is

$$\gamma_1(k_1; n) = 2l^2 \int_{k_1}^{\infty} W(l\sqrt{k^2 - k_1^2}) k^{-(n+1)} dk$$

$$\approx 2l^2 \int_{k_1}^{\infty} k^{-(n+1)} dk \text{ for } lk_1 \ll 1$$

$$\approx 2 \frac{l^2}{n} k_1^{-n} \quad 5.8$$

For large  $lk_1$ ,  $W(l\sqrt{k^2 - k_1^2}) \approx \frac{1}{l\sqrt{k^2 - k_1^2}}$

and  $\gamma_1(k_1; n) \approx 2l \int_{k_1}^{\infty} \frac{k^{-(n+1)}}{\sqrt{k^2 - k_1^2}} dk$

$$\approx lk_1^{-(n+1)} \int_0^{\infty} \frac{s^{-1} ds}{[1+s]^{\frac{n+2}{2}}}$$

$$\approx lk_1^{-(n+1)} B\left(\frac{1}{2}, \frac{n+1}{2}\right) \quad 5.9$$

The point at which asymptotes 5.8 and 5.9 meet is

$$\begin{aligned}
 \Lambda &= 2lk_1 = nB \left( \frac{1}{2}, \frac{n+1}{2} \right) \\
 &= \frac{n \Gamma(\frac{1}{2}) \Gamma(\frac{n+1}{2})}{\Gamma(\frac{n+2}{2})} \\
 &= \frac{4\Gamma(\frac{3}{2}) \Gamma(\frac{n+1}{2})}{\Gamma(\frac{n}{2})}
 \end{aligned}
 \tag{5.10}$$

Equations 5.3 and 5.10 are identical except for a factor of 2. Graph of equation 5.10 is drawn against  $n$  in Fig. 8.

The complete calculation of  $\gamma_1(k_1; 1)$  can be made by taking it in the form

$$\begin{aligned}
 \gamma_1(k_1; 1) &= \frac{1}{\pi} \iint \left( \frac{\sin k_3 l}{k_3} \right)^2 - \frac{dk_2 dk_3}{[k_1^2 + k_2^2 + k_3^2]^{3/2}} \\
 &= \frac{2l}{k_1^2} - \frac{l}{k_1^3} + \frac{l}{k_1^3} \exp[-2lk_1]
 \end{aligned}$$

as evaluated previously.

$\gamma_1(k_1; n)$  for  $n = 3, 5, 7, \dots$  can be obtained by differentiating  $\gamma_1(k_1; 1)$  with respect to  $k_1$

$$\frac{\partial \gamma_1(k_1; 1)}{\partial k_1} = -3k_1 \gamma_1(k_1; 3)$$

The ratio of measured spectrum  $\gamma_1(k_1; n)$  to the true spectrum at the point of intersection of the two asymptotes of  $\gamma_1(k_1; n)$  is plotted against  $n$  in Fig. 9.  $\gamma_1(k_1; n)$  for values of  $n$  other than 1, 3, 5, ... is obtained by extrapolation as in the case of velocity spectrum.

Graphs of the ratio of the true spectrum to the measured spectrum are drawn against the non-dimensional variable  $2lk_1$  in Fig. 11.

The present work was supported by research contract N6onr-24320. The authors would like to thank Messrs. B. T. Chu and Y. K. Pien for helpful suggestions, and Miss Patricia Clarken and Mr. Allen Gates for computing the results and drawing the figures for this report.

## REFERENCES

1. Karman, T.V. & Howarth, L., *On Statistical Theory of Isotropic Turbulence*, Proc. Roy. Soc., A194, 1938.
2. Batchelor, G.K., *The Role of Big Eddies in Homogeneous Turbulence*, Proc. Roy. Soc. A195, 1949.
3. Dryden, H. L., Schubauer, G.B., Mock, W.C. & Skramstad, H.K., *Measurements of Intensity and Scale of Wind-Tunnel Turbulence and Their Relations to the Critical Reynolds Number of Spheres*, NACA Report No. 581.
4. Frenkiel, F.N., *On The Hot-Wire Length Correction*, Phys. Rev. 75, 1263, 1949.
5. Corrsin, S. & Kovasznay, L.S.G., *On The Hot-Wire Length Correction*, Phys. Rev. 75, No. 12, 1949.
6. Weyl, F.J., *Analytical Methods in Optical Examinations of Supersonic Flow*, NAVOR. Rep. 211-45, Dec. 11, 1945.
7. Nicolesco, M., *Les Fontions Polyharmoniques, Actualités Scientifiques et Industrielles*, p. 27, Herman & Co., Paris, 1936.
8. Whittaker, E. T. and Watson, G. N., *Modern Analysis*, p. 229 Cambridge Press.
9. Kovasznay, L.S.G., *Technique for the Optical Measurement of Turbulence in High Speed Flow*. Heat Transfer and Fluid Mechanic Institute, Berkley, Calif. 1949. Published by ASME

## APPENDIX

Solution of the integral equations

$$\psi(x) = \int_x^\infty \frac{\phi(\xi)}{\xi} \frac{d\xi}{\sqrt{\xi^2 - x^2}} \quad A1$$

and

$$p(x) = \int_0^\infty q(\sqrt{x^2 + \xi^2}) d\xi \quad A2$$

Equation A2 can be reduced to A1 by the transformation  $y = \sqrt{x^2 + \xi^2}$

For the solution of A1, let  $\xi = x \csc \theta$

then 
$$\psi(x) = \frac{1}{x} \int_0^{\pi/2} \phi(x \csc \theta) d\theta$$

This equation can be reduced to Schlömilch equation by the transformation

$$x = \frac{1}{y}$$

let 
$$\frac{\psi(\frac{1}{y})}{y} = \Psi(y) \text{ and } \phi(\frac{1}{y}) = \Phi(y)$$

$$\Psi(y) = \int_0^{\pi/2} \Phi(y \sin \theta) d\theta$$

Solution of Schlömilch equation is<sup>8</sup>

$$\Phi(y) = \frac{2}{\pi} [\Psi(y)]_{y=0} + \frac{2}{\pi} y \int_0^{\pi/2} \Psi'(y \sin \theta) d\theta$$

or in terms of the original variables

$$\phi(x) = \frac{2}{\pi} [x \psi(x)]_{x=\infty} - \frac{2}{\pi} x \int_0^{\pi/2} [x \csc \theta \psi(x \csc \theta)]' \csc^2 \theta d\theta$$

$$\phi(x) = - \frac{2}{\pi} \int_x^\infty [\xi \psi(\xi)]' \frac{\xi d\xi}{\sqrt{\xi^2 - x^2}} \quad A3$$

Alternatively,

$$\psi(x) = \int_x^\infty \frac{\phi(\xi) d\xi}{\xi \sqrt{\xi^2 - x^2}}$$

can be solved by the transformation

$$\begin{aligned}\xi &= \frac{1}{\sqrt{\xi_1}} \\ x &= \frac{1}{\sqrt{x_1}} \\ \phi(\xi) &= \phi\left(\frac{1}{\sqrt{\xi_1}}\right) = \bar{\phi}(\xi_1) \\ \psi(x) &= \psi\left(\frac{1}{\sqrt{x_1}}\right) = \bar{\psi}(x_1)\end{aligned}$$

Substituting these in our equation we get Abel integral equation.

$$\frac{\bar{\psi}(x_1)}{\sqrt{x_1}} = \frac{1}{2} \int_0^{x_1} \frac{\bar{\phi}(\xi_1)}{\sqrt{\xi_1}} \frac{d\xi_1}{\sqrt{x_1 - \xi_1}}$$

Its solution is<sup>8</sup>:

$$\frac{\frac{1}{2} \bar{\phi}(x_1)}{\sqrt{x_1}} = \frac{1}{\pi} \frac{d}{dx_1} \int_0^{x_1} \frac{\bar{\psi}(\xi_1) d\xi_1}{\sqrt{\xi_1} \sqrt{x_1 - \xi_1}}$$

or in terms of original variables

$$\varphi(x) = \frac{-2}{\pi} x^2 \frac{d}{dx} x \int_x^\infty \frac{\psi(\xi) d\xi}{\xi \sqrt{\xi^2 - x^2}}$$

A4

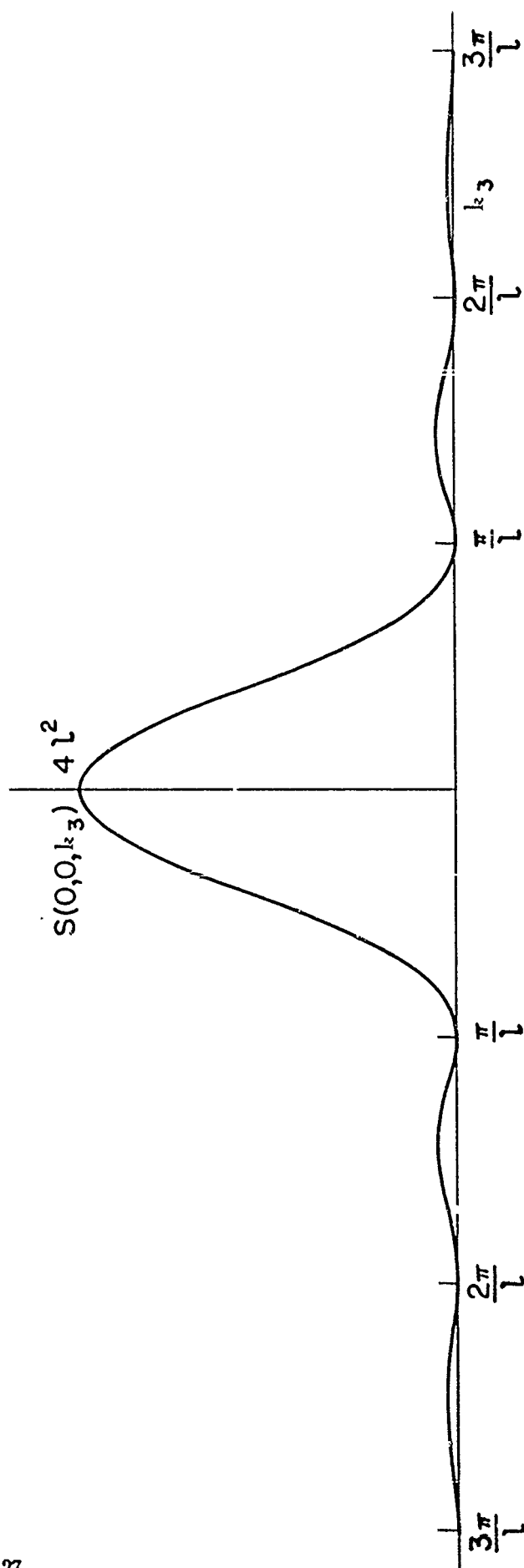
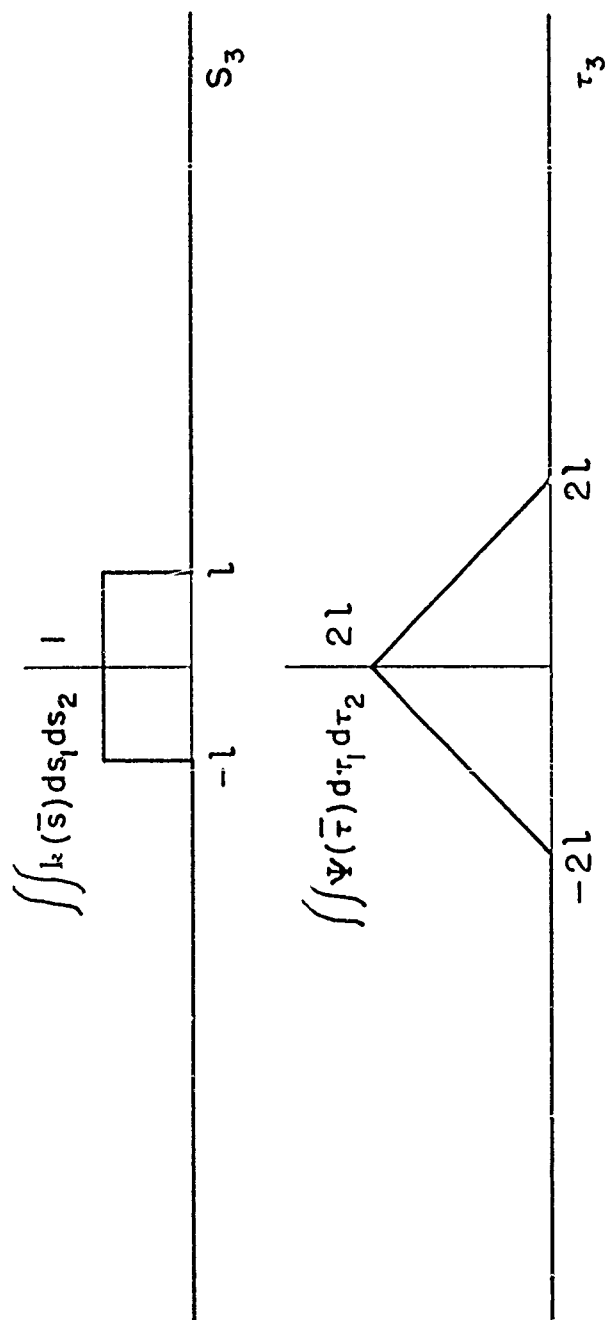


Figure 1 — Functions characterizing the response of a hot wire of length  $2l$

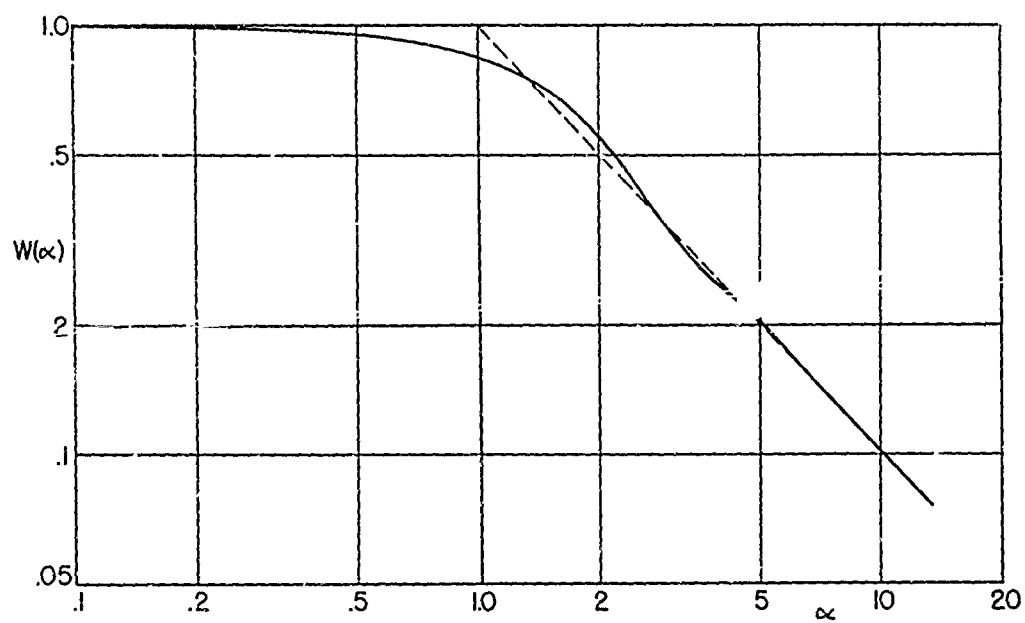


Figure 2 — The function  $W(\alpha)$

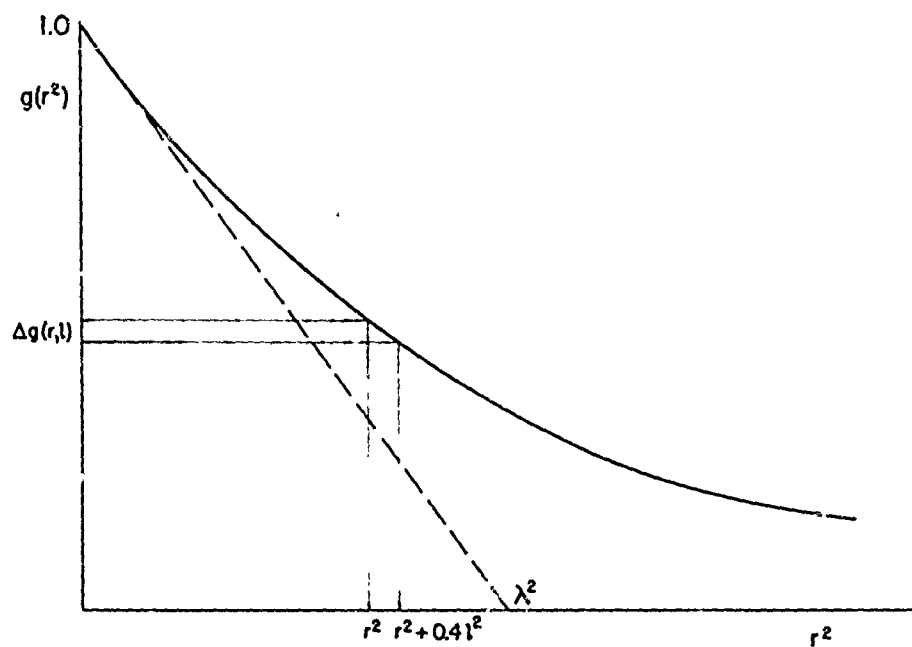


Figure 3 — Illustration of simple approximate method of correcting lateral correlation.



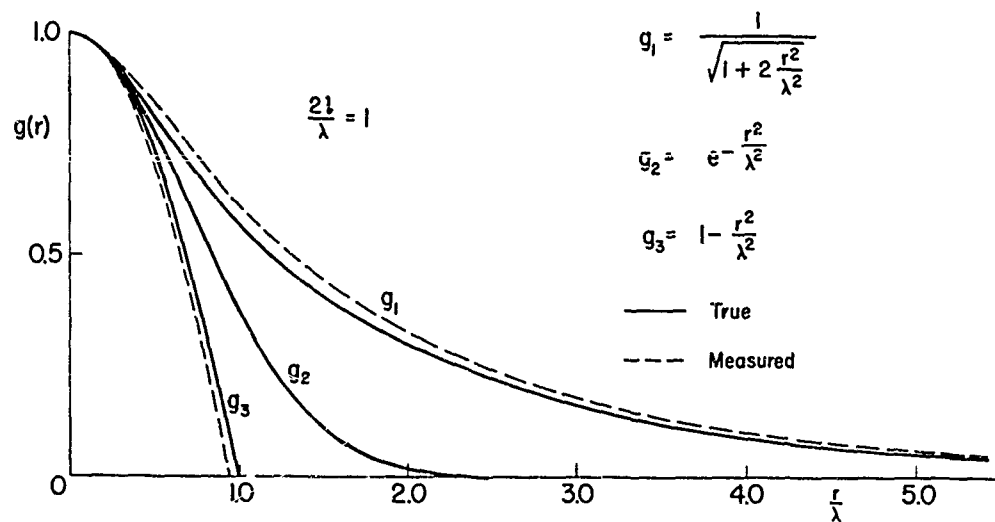


Figure 4 — Effect of finite resolution on lateral correlation measurements.

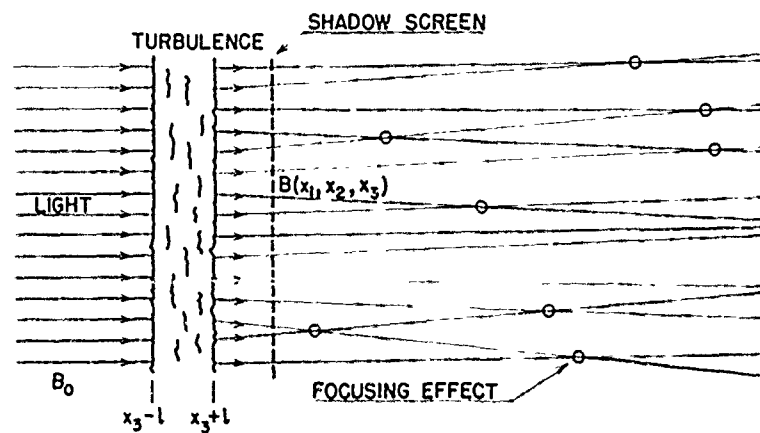


Figure 5 — Optical arrangement for taking shadow pictures.

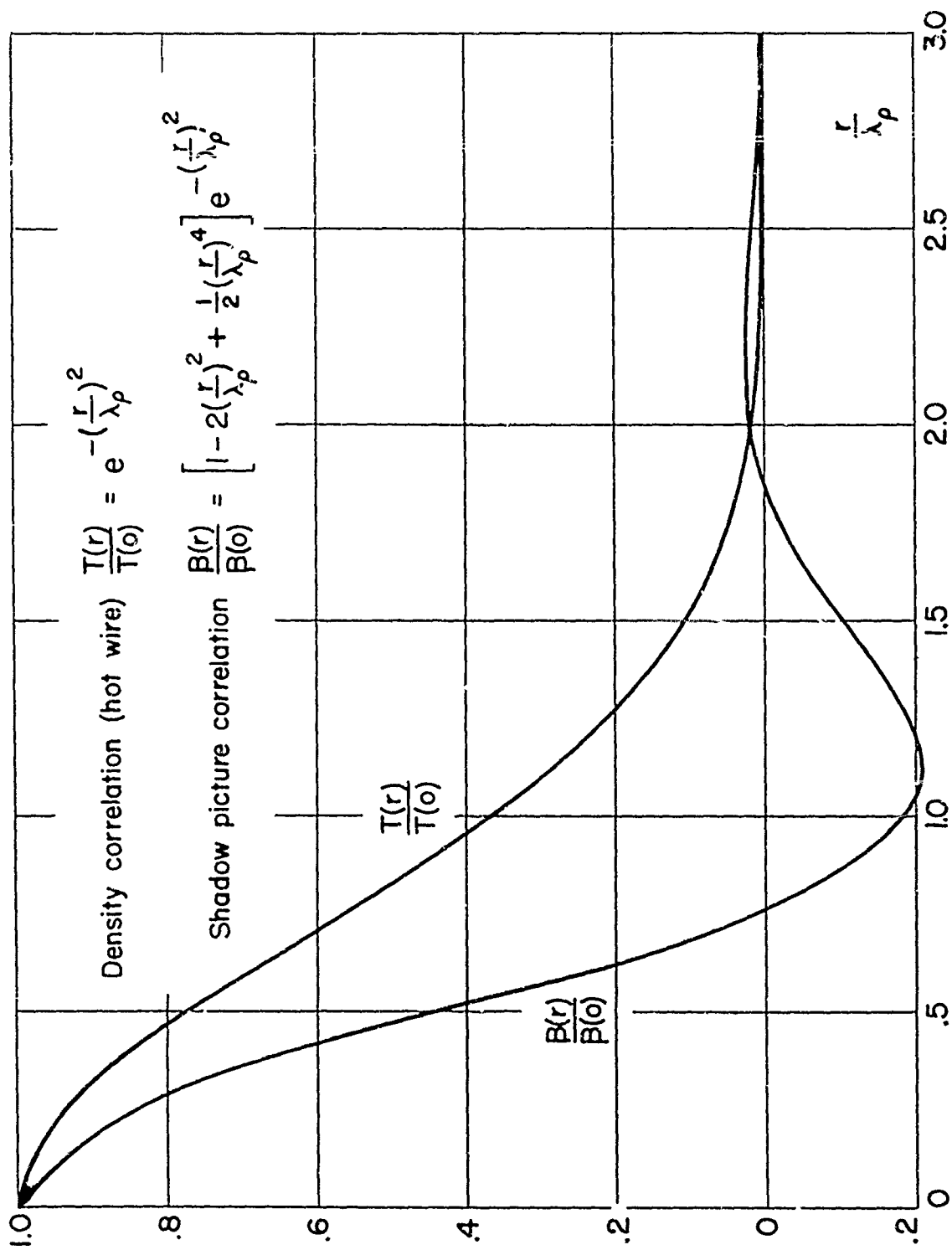


Figure 6 — Correlation coefficient of density fluctuations compared with the correlation coefficient of the shadow picture (isotropic turbulence).

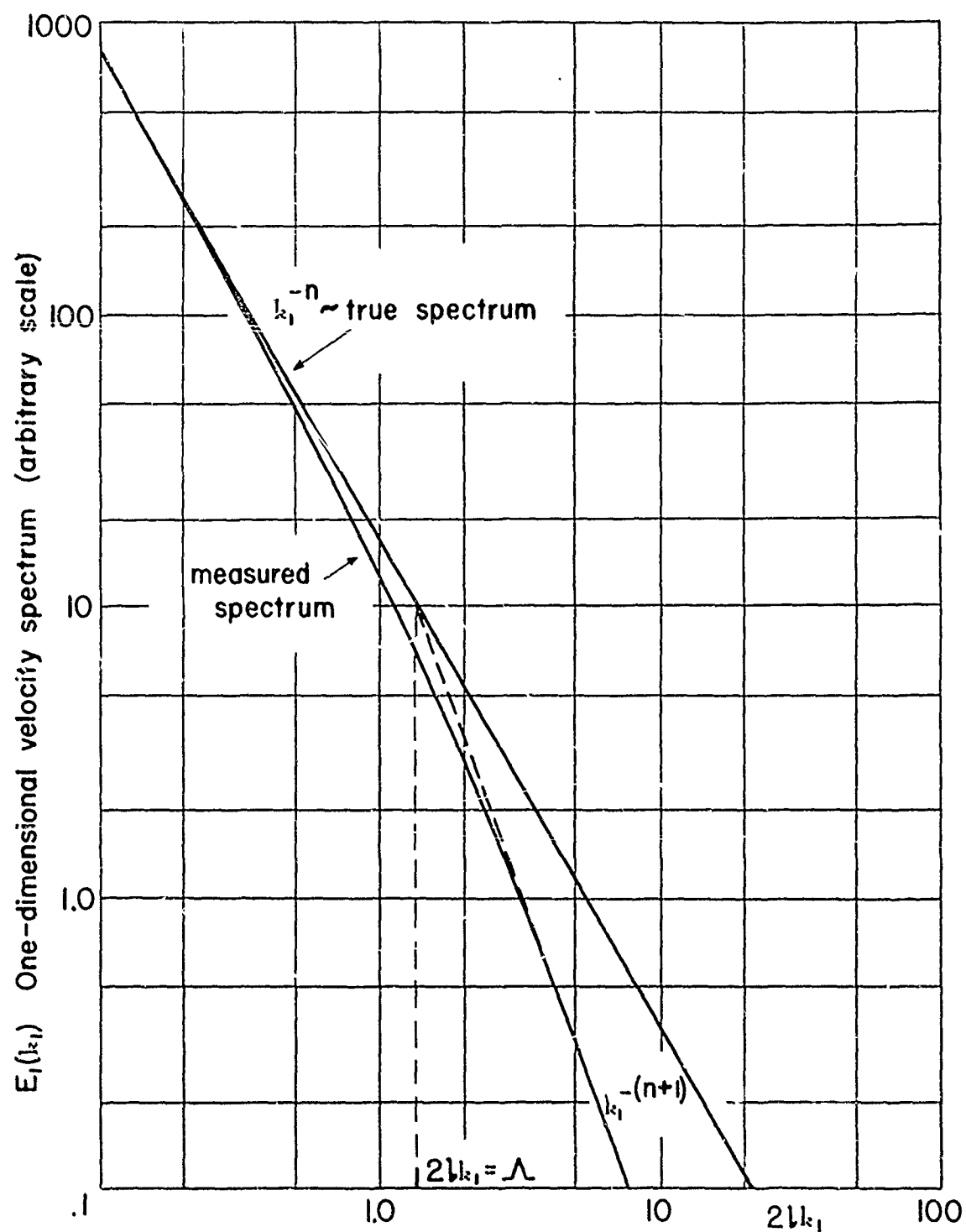


Figure 7 — Effect of finite wire length on velocity power spectrum. True spectrum assumed  $E_1(k_1) \sim k_1^{-n}$  (in figure  $n = \frac{5}{3}$ , at intersection of asymptotes  $2lk_1 = \Lambda$ ).

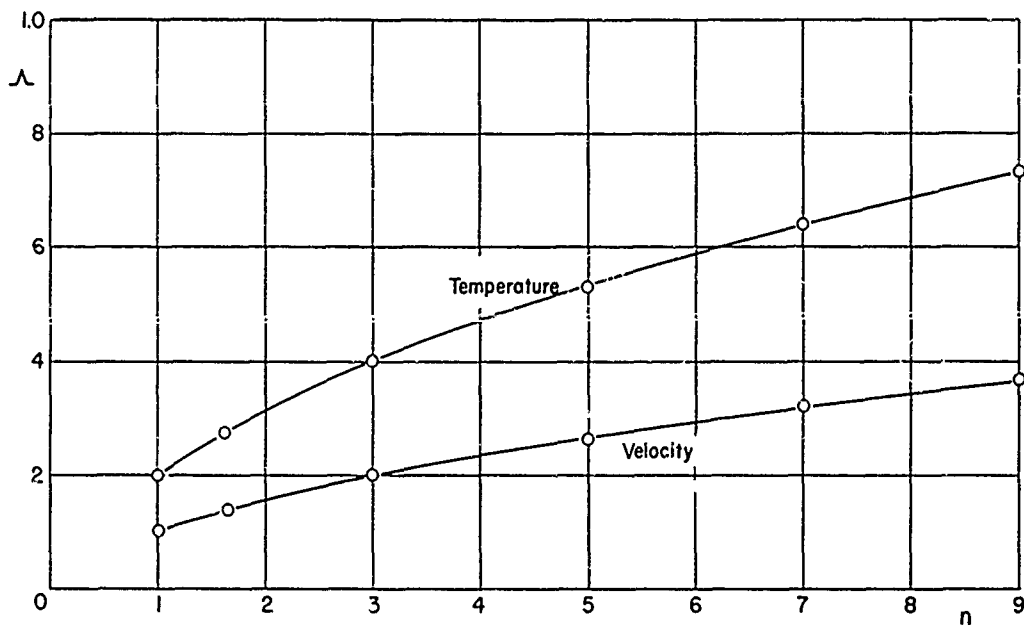


Figure 8 — Intersection of asymptotes in measured spectrum (see Fig. 7)

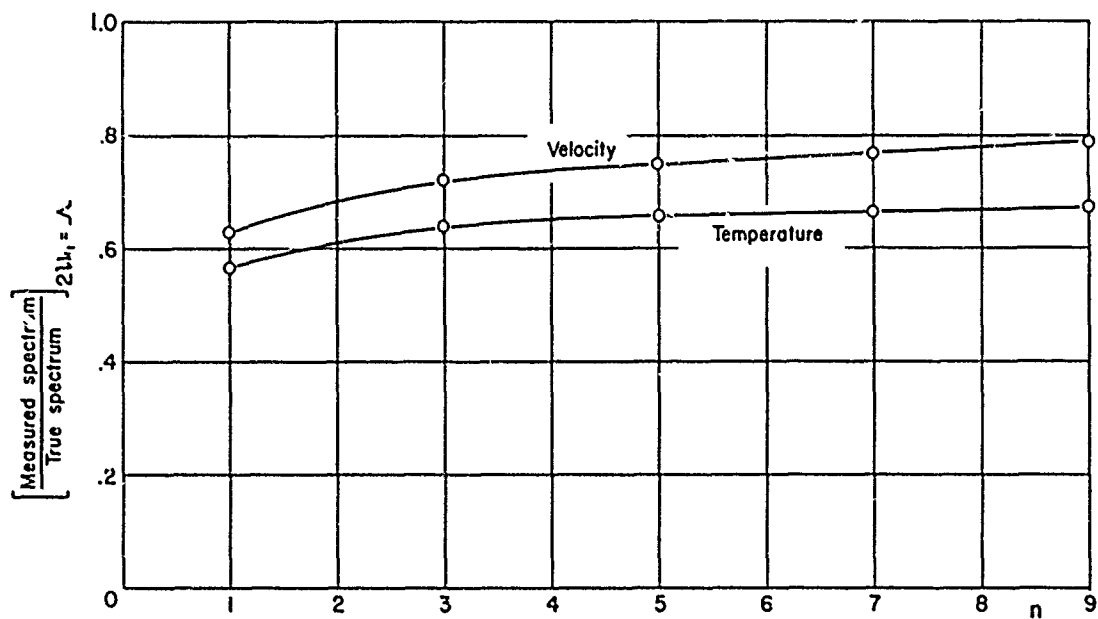


Figure 9 — Ratio of measured spectrum to true spectrum at the point of intersection of asymptotes.

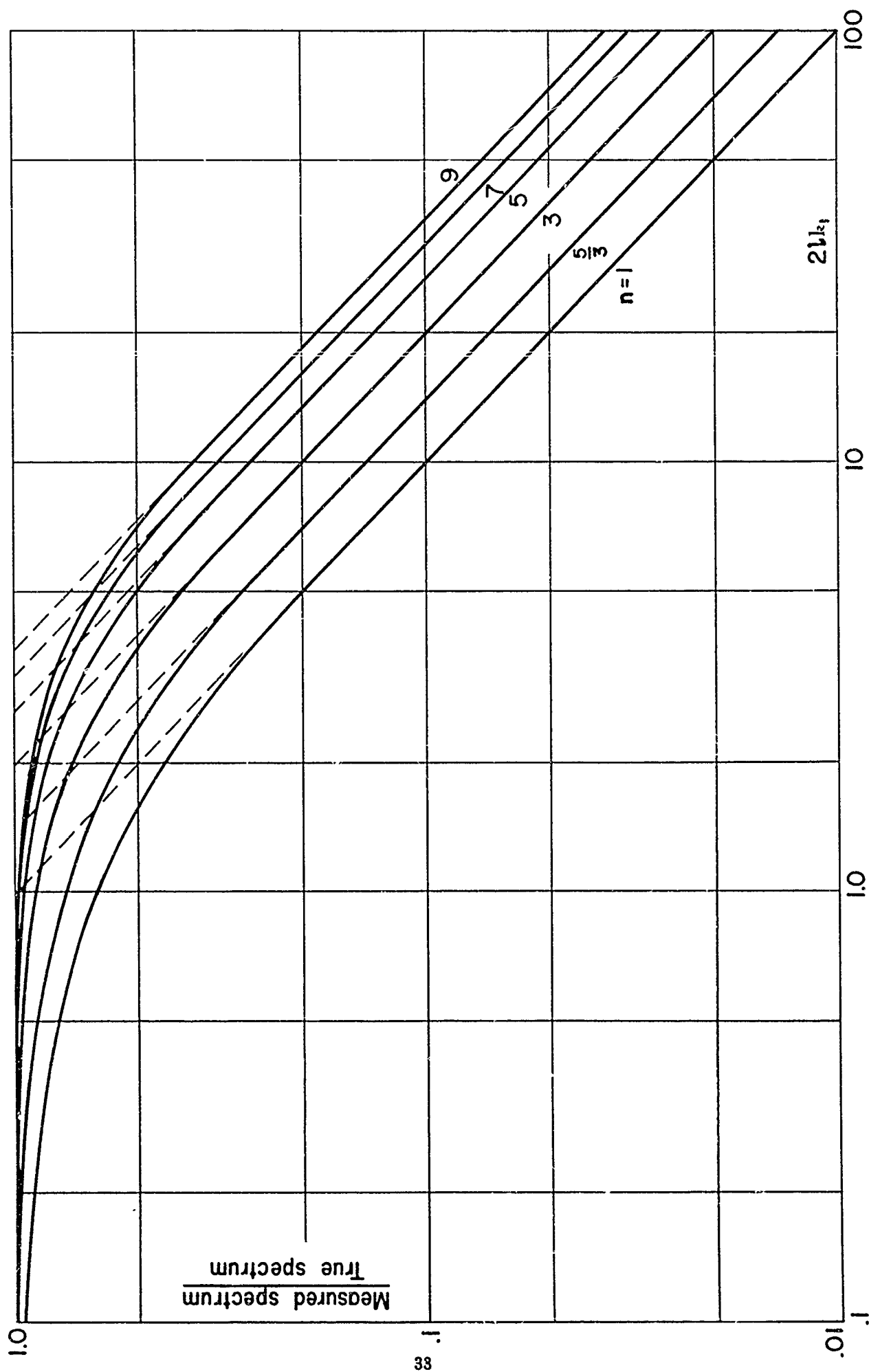


Figure 10 — Effect of finite resolution on some simple velocity spectra.

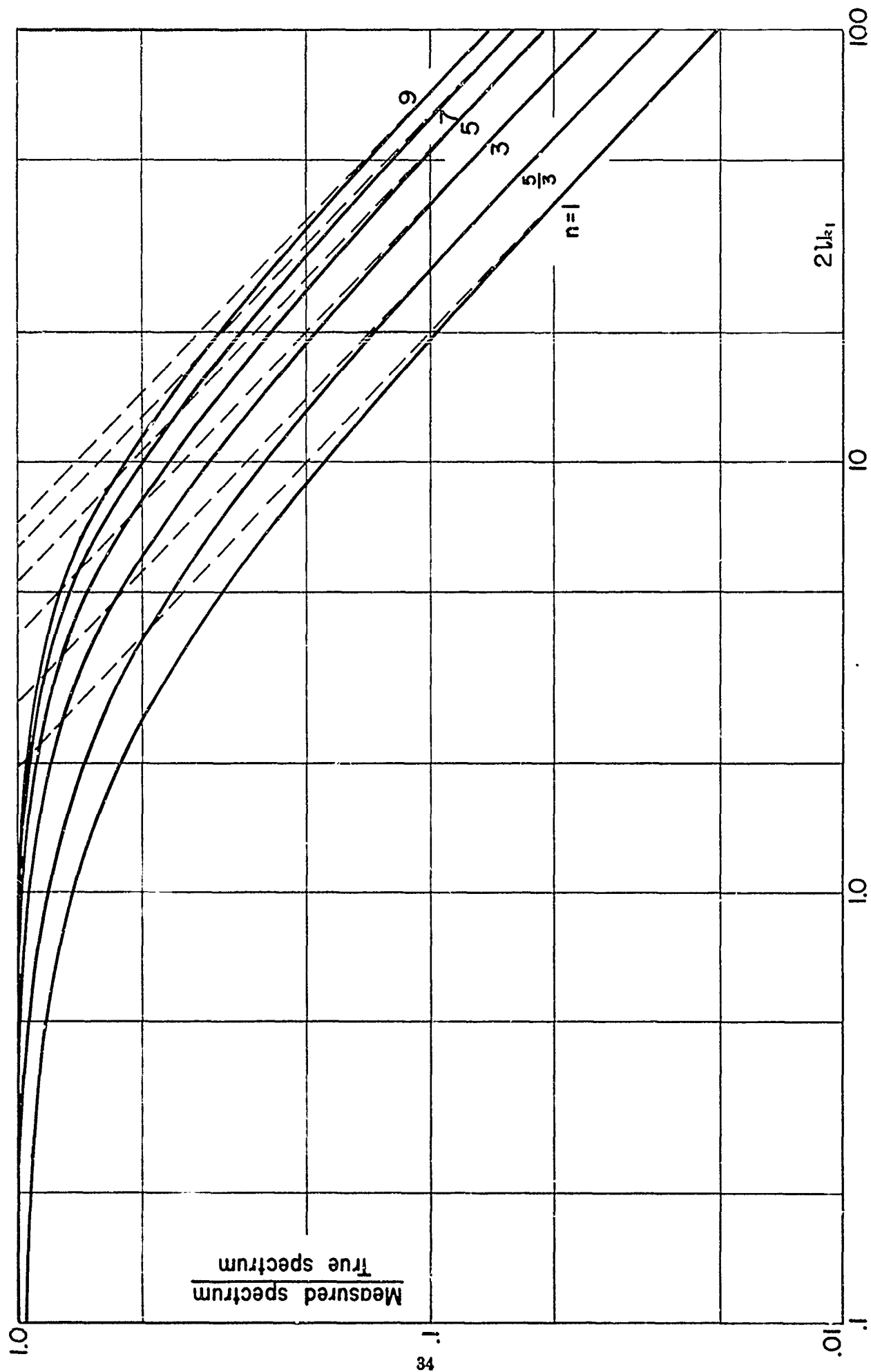


Figure II — Effect of finite resolution on some simple temperature spectra.

## PROJECT SQUID DISTRIBUTION LIST

PARTS A, B, C, AND DP of the A.N.A.F.G.M. Mailing List, July, 1951 Also, Project SQUID list:

1. H. S. Taylor, Princeton University
2. J. V. Charyk, Princeton University
3. F. Clauser, Johns Hopkins University
4. J. V. Foa, Cornell Aeronautical Laboratory
5. N. J. Hoff, Polytechnic Institute of Brooklyn
6. G. E. Hudson, New York University
7. M. W. Woody, New York University
8. M. J. Zucrow, Purdue University
9. K. Wohl, University of Delaware
10. G. Markstein, Cornell Aeronautical Laboratory
11. R. N. Pease, Princeton University
12. P. Libby, Polytechnic Institute of Brooklyn
13. S. A. Guerrieri, University of Delaware
14. L. Lees, Princeton University
15. G. Rudinger, Cornell Aeronautical Laboratory
16. J. M. Smith, Purdue University
17. S. W. Yuan, Aerojet Engineering Corporation
18. J. H. Hett, New York University
19. M. J. Storm, New York University
20. P. K. Porter, Cornell Aeronautical Laboratory
21. H. J. Yearian, Purdue University
22. J. T. Grey, Cornell Aeronautical Laboratory
23. H. J. Shafer, Princeton University
24. A. P. Colburn, University of Delaware
25. G. S. Meikle, Purdue University
26. J. J. O'Neil, Cornell Aeronautical Laboratory
27. R. J. Woodrow, Princeton University
28. H. K. Work, New York University
29. A. Kahane, Princeton University
30. F. A. Parker, Princeton University
31. M. Summerfield, Princeton University
32. W. J. Barr, Princeton University
33. J. H. Wakelin, Textile Research Foundation
- 34/46. Chief of Naval Research, Code 429, Washington, D. C. (13 cc)
47. Commanding Officer, O.N.R., New York, New York
48. Commanding Officer, O.N.R., Chicago, Illinois
49. Commanding Officer, O.N.R., Boston, Massachusetts
50. Commanding Officer, O.N.R., San Francisco, California
51. Commanding Officer, O.N.R., Pasadena, California
- 52/55. Chief, Bureau of Aeronautics, Power Plant Div., Exp. Engines Branch (3)
56. Chief, Bureau of Aeronautics, Power Plant Div., Fuels & Lubricants Branch
57. Chief, Bureau of Aeronautics, Ship Installations Div.
58. P. Kratz, O.N.R. Res. Representative, Philadelphia, Pennsylvania
59. Commander R.W. Pickard, BuAer Representative, Cornell Aeronautical Laboratory, Buffalo, New York
60. D. G. Samaras, Office of Air Research, Wright-Patterson Air Force Base
- 61/62. F. Tanczos, Bureau of Ordnance, Guided Missiles Division, Washington
63. W. Worth, Power Plant Laboratory, Engineering Div., Wright Field
64. C. F. Yost, Directorate of Research & Development, USAF, Pentagon

- 65/66. Chief of Naval Research, Navy Research Section, Library of Congress
67. W. Tenney, Aeromarine Company
68. R. Folsom, University of California, Mechanical Engineering Department
69. Engineering Librarian, Columbia University Library
70. C. Millikan, Guggenheim Aeronautical Laboratory, California Institute of Technology
71. B. L. Crawford, Department of Chemistry, University of Minnesota
72. Officer in Charge, Naval Ordnance Test Station, Pasadena, California
73. J. Moriarty, Purdue University Library
74. B. Lewis, Bureau of Mines, Pittsburgh, Pennsylvania
75. L. Crocco, Princeton University
76. Manson Benedict, Hydrocarbon Research, Inc., New York City
77. Gerhard Dieke, Johns Hopkins University
78. M. W. Evans, 3115 Western Avenue, Park Forest, Chicago Heights, Illinois
79. K. F. Herzfeld, Department of Physics, Catholic University of America
80. Arnold Kuethe, University of Michigan, Ann Arbor, Michigan
81. C. C. Lin, Dept. of Aero. Engg., Massachusetts Institute of Technology
82. G. H. Messerly, Special Products Dept., M. W. Kellogg Co., Jersey City
83. A. J. Nerad, Consulting Engineering Lab., General Electric, Schenectady
84. W. R. Sears, Grad. School of Aero. Engg., Cornell University
85. Gunther von Elbe, U. S. Bureau of Mines, Central Exp. Station, Pittsburgh
86. G. Henning, Aerojet Engineering Corp., Azusa, California
87. J. B. Henry, Allegheny Ludlum Steel Corp., Breckenridge, Pennsylvania
88. L. N. K. Boelter, University of California, Los Angeles, California
89. Committee on Undersea Warfare, National Research Council, Washington
90. P. A. Lagerstrom, Guggenheim Aero. Lab., California Institute of Technology
91. J. Keenan, Massachusetts Institute of Technology, Cambridge, Massachusetts
92. J. D. Akerman, University of Minnesota, Minneapolis, Minnesota
93. W. A. Wildhack, National Bureau of Standards, Washington, D. C.
94. Buffalo-Electro Chemical Corporation, Buffalo, New York
95. R. Ladenburg, Princeton University, Physics Department
96. D. H. Hill Library, University of North Carolina, Raleigh, North Carolina
97. I.T.E.-Circuit Breaker Company, Special Products Div., Philadelphia, Pa.
98. Aircooled Motors, Inc., Syracuse, New York
99. AirResearch Manufacturing Company, Los Angeles, California
100. Allison Division, General Motors Corporation, Indianapolis, Indiana
101. B. G. Corporation, New York 19, New York
102. Champion Spark Plug Company, Toledo, Ohio
103. Fredric Flader, Inc., North Tonawanda, New York
104. General Electric Company, Aircraft Gas Turbines Div., West Lynn, Mass.
105. General Laboratory Associates, Inc., Norwich, New York
106. Lycoming-Spencer Div., Avco Manufacturing Corporation, Williamsport, Pa.
107. McCulloch Motors Corporation, Los Angeles, California
108. Pratt and Whitney Aircraft Division, U.A.C., East Hartford, Connecticut
109. Stalker Development Company, Bay City, Michigan
110. Stanford University, Stanford California
111. Thompson Products Inc., Cleveland, Ohio
112. University of Southern California, Los Angeles, California
113. Westinghouse Electric Corporation, A.G.T. Division, Essington, Pa.
114. Kenneth Razak, Acting Dean, College of Business Administration and Industry, University of Wichita,  
Wichita, Kansas
- 115/117. Cornell Aeronautical Library, 4455 Genesee Street, Buffalo, N.Y. (3cc)
118. Georgia Institute of Technology, Dept. of Mech. Engin., Attn. Prof. M. J. Goglia



#### ABSTRACT

Functional relations are derived between the true correlations and spectra of a random field and those measured with a probe of finite resolving power. The case of a probe having zero resolving power in one direction (e.g. infinitely long hot-wire) is examined and it is shown that in the case of homogeneous random fields, the true correlations and spectra can be recovered from the corresponding measured quantities. These relations are applied to turbulence measurements by hot-wire anemometer and optical methods. Explicit calculations of hot-wire length effect are made for some simple velocity and temperature spectra.

#### ABSTRACT

Functional relations are derived between the true correlations and spectra of a random field and those measured with a probe of finite resolving power. The case of a probe having zero resolving power in one direction (e.g. infinitely long hot-wire) is examined and it is shown that in the case of homogeneous random fields, the true correlations and spectra can be recovered from the corresponding measured quantities. These relations are applied to turbulence measurements by hot-wire anemometer and optical methods. Explicit calculations of hot-wire length effect are made for some simple velocity and temperature spectra.

#### ABSTRACT

Functional relations are derived between the true correlations and spectra of a random field and those measured with a probe of finite resolving power. The case of a probe having zero resolving power in one direction (e.g. infinitely long hot-wire) is examined and it is shown that in the case of homogeneous random fields, the true correlations and spectra can be recovered from the corresponding measured quantities. These relations are applied to turbulence measurements by hot-wire anemometer and optical methods. Explicit calculations of hot-wire length effect are made for some simple velocity and temperature spectra.

#### ABSTRACT

Functional relations are derived between the true correlations and spectra of a random field and those measured with a probe of finite resolving power. The case of a probe having zero resolving power in one direction (e.g. infinitely long hot-wire) is examined and it is shown that in the case of homogeneous random fields, the true correlations and spectra can be recovered from the corresponding measured quantities. These relations are applied to turbulence measurements by hot-wire anemometer and optical methods. Explicit calculations of hot-wire length effect are made for some simple velocity and temperature spectra.

INFLUENCE OF RESOLVING POWER ON MEASUREMENT  
OF CORRELATIONS AND SPECTRA OF RANDOM FIELDS

by

Mahinder S. Uberoi and Leslie S. G. Kovásznaý

Johns Hopkins University  
Baltimore, Maryland

Project Squid Technical Report No. 30

*(Abstract on Reverse Side)*

INFLUENCE OF RESOLVING POWER ON MEASUREMENT  
OF CORRELATIONS AND SPECTRA OF RANDOM FIELDS

by

Mahinder S. Uberoi and Leslie S. G. Kovásznaý

Johns Hopkins University  
Baltimore, Maryland

Project Squid Technical Report No. 30

*(Abstract on Reverse Side)*

INFLUENCE OF RESOLVING POWER ON MEASUREMENT  
OF CORRELATIONS AND SPECTRA OF RANDOM FIELDS

by

Mahinder S. Uberoi and Leslie S. G. Kovásznaý

Johns Hopkins University  
Baltimore, Maryland

Project Squid Technical Report No. 30

*(Abstract on Reverse Side)*

INFLUENCE OF RESOLVING POWER ON MEASUREMENT  
OF CORRELATIONS AND SPECTRA OF RANDOM FIELDS

by

Mahinder S. Uberoi and Leslie S. G. Kovásznaý

Johns Hopkins University  
Baltimore, Maryland

Project Squid Technical Report No. 30

*(Abstract on Reverse Side)*